UNIVERSITI TEKNIKAL MALAYSIA MELAKA

STRUCTURAL INTEGRITY ASSESSMENT OF CABLE/STRUCTURE :FROM LABORATORY TO INDUSTY

NURUL FAHIMAH BINTI AFANDI

BACHELOR OF MECHANICAL ENGINEERING TECHNOLOGY (BMMV) WITH HONOURS

2023

UNIVERSITI TEKNIKAL MALAYSIA MELAKA

Faculty of Mechanical and Manufacturing Engineering Technology

STRUCTURAL INTEGRITY ASSESSMENT OF CABLE/STRUCTURE :FROM LABORATORY TO INDUSTY

Nurul Fahimah Binti Afandi

Bachelor of Mechanica Engineering Technology (BMMV) with Honours

2023

STRUCTURAL INTEGRITY ASSESSMENT OF CABLE/STRUCTURE :FROM LABORATORY TO INDUSTY

NURUL FAHIMAH BINTI AFANDI

A thesis submitted
in fulfillment of the requirements for the degree of
Bachelor of Mechanical Engineering Technology (BMMV) with Honours

Faculty of Mechanical and Manufacturing Engineering Technology

UNIVERSITI TEKNIKAL MALAYSIA MELAKA

2023

DECLARATION

I declare that this Choose an item. entitled " STRUCTURAL INTEGRITY ASSESSMENT OF CABLE/STRUCTURE : FROM LABORATORY TO INDUSTRY " is the result of my own research except as cited in the references. The STRUCTURAL INTEGRITY ASSESSMENT OF CABLE/STRUCTURE : FROM LABORATORY TO INDUSTRY has not been accepted for any degree and is not concurrently submitted in candidature of any other degree.

Signature :

Name : NURUL FAHIMAH BINTI AFANDI

Date : 11/01/2023

APPROVAL

I hereby declare that I have checked this thesis and in my opinion, this thesis is adequate in terms of scope and quality for the award of the Bachelor of Mechanical Engineering Technology (BMMV) with Honours.

Signature :

Supervisor Name : EN.FEBRIAN BIN IDRAL

Date : 11/1/2023

DEDICATION

My dissertation is loving parents and many friends. Particular thanks to my dear parents, Afandi and Madusiah, whose words of support and persistence continue to ring in my ears. Fahirani, Fazizatul, Fazana, and Farisha, my four sisters, never once have left my side and are very dear to me. This dissertation is also dedicated to my numerous friends who have helped me during the process. I will always be grateful and all they've done for me, especially Afiq's assistance in developing my technological abilities and Amirul's many hours of proofreading. I dedicate this work to my dearest friend Atiqah and Imtinah, and I thank them who will be there for me throughout my Degree programme. You've both been my biggest supporters.

ABSTRACT

Within engineering and building projects, strain and displacement are significant characteristics. Outside of the lab, however, measuring these parameters necessitates a tough choice between established procedures, as precision, simplicity, and cost must all be considered. Digital Imaging Correlation (DIC) is a technique that has the potential to be great for studying crack propagation and structural deformation in real-world applications since it is a cheap, easy, and precise solution. DIC has traditionally been used on grayscale photos captured with monochromatic cameras, but with the development of digital colour cameras, Color DIC may now be used on colour images.Color pictures are predicted to provide more information, hence the same subset size for Color DIC should produce better results than typical grayscale DIC. The influence of varying sizes of speckles in speckle patterns and different forms of deformation on the performance of Color DIC and grayscale DIC is investigated in this study. Images were numerically created and speckle patterns and deformations were simulated. The findings imply that, in general, colour DIC produces superior outcomes than grayscale DIC. The amount of improvement in Color DIC performance is determined on the size of the speckles that escape the image and the type of deformation. In most cases, improvement is greatest for small subset sizes and diminishes as the subset size grows larger.It was also discovered that for complicated and nuanced deformation circumstances, grayscale DIC outperforms colour DIC if the selected subset is greater than a specified subset size, commonly referred to as "ideal subset size."

ABSTRAK

Terikan dan anjakan adalah merupakan ciri yang paling penting dalam projek kejuruteraan dan bangunan. Mengukur parameter ini di luar makmal memerlukan pilihan yang amat sukar antara prosedur yang telah ditetapkan, kerana ketepatan, kesederhanaan, dan kos mesti dipertimbangkan. Korelasi Pengimejan Digital (DIC) merupakan penyelesaian yang murah, mudah, dan tepat untuk mengkaji perambatan retak dan ubah bentuk struktur dalam aplikasi dunia sebenar. Warna DIC kini boleh digunakan pada imej berwarna dengan pembangunan kamera warna digital. DIC secara traditional telah digunakan pada photo skala kelabu yang ditangkap dengan kamera monokromatik, tetapi dengan pembangunan kamera warna digital, gambar berwarna dapat diramalkan dan memberi lebih banyak maklumat, oleh itu saiz subset yang sama untuk warna DIC sepatutnya menghasilkan keputusan yang lebih baik daripada DIC skala kelabu biasa. Pengaruh pelbagai saiz bintik dalam corak bintik dan bentuk ubah bentuk yang berbeza terhadap prestasi DIC Warna dan DIC skala kelabu disiasat dalam kajian ini. Imej telah dicipta secara berangka dan corak bintik dan ubah bentuk telah disimulasikan. Penemuan menunjukkan bahawa, secara amnya, DIC berwarna menghasilkan hasil yang lebih baik daripada DIC skala kelabu. Jumlah peningkatan dalam prestasi DIC Warna ditentukan pada saiz bintik-bintik yang terlepas daripada imej dan jenis ubah bentuk. Dalam kebanyakan kes, penambahbaikan adalah yang terbaik untuk saiz subset yang kecil dan berkurangan apabila saiz subset semakin besar. Ia juga mendapati bahawa untuk keadaan ubah bentuk yang rumit dan bernuansa, DIC skala kelabu mengatasi DIC warna jika subset yang dipilih lebih besar daripada saiz subset yang ditentukan, biasanya dirujuk sebagai "saiz subset yang ideal."

ACKNOWLEDGEMENTS

In the Name of Allah, the Most Gracious, the Most Merciful

First and foremost, I'd like to express my gratitude and praise to Allah the Almighty, my Creator, for everything I've been given since the beginning of my life. I'd like to express my gratitude to Universiti Teknikal Malaysia Melaka (UTeM) for providing the research environment. Thank you also for the financial support from the Malaysian Ministry of Higher Education (MOHE).

En. Febrian Bin Idral, Lecture of Engineering Technology Department (UTeM), is my primary supervisor, and I am grateful for all of his help, advise, and motivation. His unwavering patience in guiding and imparting priceless insights will be remembered for the rest of his life.Also, to my co-supervisor, Ts. Dr. Ahmad Fuad Bin Ab Ghani, Universiti Teknikal Malaysia Melaka (UTeM) who constantly supported my journey.

Last but not least, I want to express my gratitude to Muhammad, one of my coworkers, for his encouragement and for being a pillar of strength in all of my undertakings.I'd also like to express my gratitude to my loving parents for their unwavering support, love, and prayers. Finally, I'd like to express my gratitude to everyone who has helped, supported, and inspired me to pursue my studies

TABLE OF CONTENTS

PAGE

DECLARATION

APPROVAL

DEDICATION

LIST OF TABLES

TABLE **TITLE** **PAGE**

LIST OF FIGURES

FIGURE **TITLE** **PAGE**

LIST OF SYMBOLS AND ABBREVIATIONS

D,d - Diameter

DIC - Digital Image Correlation

2-D - 2 Dimensional

σ - Stress

A - Area

F - Force

ε - Strain

- Difference of Length

- Length

LIST OF APPENDICES

APPENDIX **TITLE** **PAGE**

CHAPTER 1

INTRODUCTION

1.1 Background

DIC or known as digital image correlation is a non-contact technique for capturing an image on a project surface area using the high speed camera to undertake the image analysis investigations to obtain patterns of deformation modifications and measurements. It employs the optical approach, which involves tracking and registration the image for precision and accuracy in 2D and 3D which are fixed in the event of a change in the image. This method is widely used, particularly in the domains of the engineering and science. The measuring of distortion in a section of a material is critical in engineering, especially when dealing with external loads.

A research group at the University of South Carolina has been developing a method for measuring surface deformation using digital image correlation methods since the 1980s. After that, several researchers modified the approach to improve resolution, accuracy, and solve the disadvantages mentioned above. This technology is now used to solve a variety of problems, including structural mechanics, high-temperature deformation measurement, biomaterials, wood products, and inverse stress analysis. In latest days, this technique has begun to be applied to deformation measurement which use pictures from SEM, AFM, and X-ray microtomography.

The high-speed camera will be angled at 90 degrees to the cable or rope to complete this process. Changes in the cable will be captured and transformed into photos. After that, the image will be loaded into the MATLAB and DIC programme. The image will undergo modifications that the DIC may detect in terms of deformation, contour, and other factors.

The fundamental principle of digital image correlation is presented in this article. The method's efficiency is then demonstrated by measuring the displacement field toward the cable or rope using the procedure. All of the data, such as yield strength, will be calculated using the value strain obtained through the DIC approach. Because the measurement can be done quickly and easily, the technology is predicted to be widely used in a variety of fields.

1.2 Problem Statement

The evaluation of a material structure is critical when choosing the right material for a certain sector. The material's deformation can be seen with the naked eye, but it's impossible to tell how the material deforms from phase to phase until it's deformed. Although the most up-to-date technology can operate the material, it is prohibitively expensive for a small business to own.

An analytical study on ropes or cables used in industry will be conducted using digital image correlation (DIC). With these findings, it will be possible to integrate DIC into the market as well as develop appropriate tools for industrial usage in trying to analyse material performance.

1.3 Research Objective

The main aim of this research is to analyse the data deformation of material and its characterization. Specifically, the objectives are as follows:

a) To apply the image from high speed camera for the digital image correlation(DIC).

b) To implemented the deformation and strain analysis using the digital image correlation(DIC) method.

1.4 Scope of Research

The application of digital image correlation (DIC) in the investigation of material structure (rope/cable) is the focus of this research. Numerous tests, such as the izod test, the charpy test, and others, have been used to explore the material's structure for a long time. The industrial sector may acknowledge the utility of DIC in appraising materials and structural durability testing in the future. Deformation on the cable will be done using digital image correlation to ensure that the DIC can be used to produce values and deformation parameters for each mechanical structure.

CHAPTER 2

LITERATURE REVIEW

2.1 Introduction

Design, selection, and characterization of materials, as well as stress and failure analysis, are all parts of structural integrity(Felippa, 2004). Additive manufacturing, non-damage assessment, fracture mechanics, and damage are all examples of material characterization and processing. Material characterization is critical in the engineering industry because it uses a large number of materials in every structure of public-use items(A. F. Ab Ghani et al., 2016). Each material has its own level of durability and application. A product's future difficulties will be caused by improper material choices. Many factors need to be taken while evaluating materials to ensure that the material's performance is safe to use, including yield strength, deformation, structural rigidity, and others(Górszczyk et al., 2019).

Each material has it own characteristic depend to their own capability to undergo the test of failure. To be identified the material characteristic, there would be many test that can be done to able to determine it (Tavares, 2015). For example, in the laboratory, one can make a tensile test to determine the tensile value for each material that need to be study (Felippa, 2004). Based on the value that obtain from each experiment, needs to do some calculation for the stress and strain.

The purpose to obtain those stress and strain data were important as it can identify the material durability to certain load that apply to it (Motamedi, 2019). So that, this can be a safety measurement for engineer to improvise the product for the future planning. In this modern technology, there were many method that can be used to run the analysis for each material strength such as SolidWork software, Catia and many else (Felippa, 2004). In this case study is to use the Digital Image Correlation (DIC) to run the analysis. Hence, there also many methods that can be used such as:

2.2 Moire Techniques

The moire method is a technique for determining material stress and strain. The principle of in-plane moire method is a principle that is related to this moire method (Melin, 1995). The in-plane Moire fringes are formed by the interference of two sets of gratings that are in direct contact. The gratings are created to order and are arranged in high density, dark, and light bands. The range between any of the two grating pitches, each of which was labelled "p." Typically, the grating lines are parallel and facing each other in a straight state. However, forming the grating line in a circular condition is not impossible (Eindhoven et al., 2022)

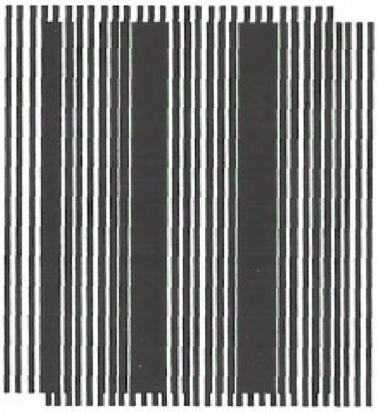

Figure 2.1 Moire between two grating with different pitch

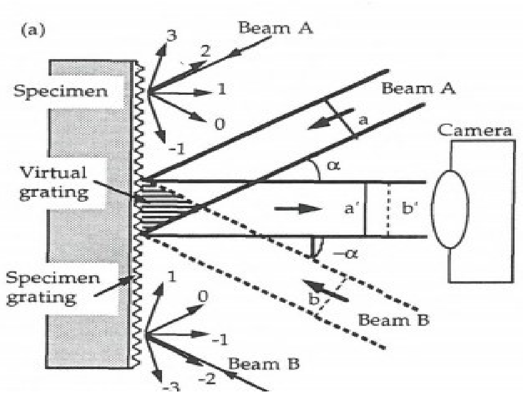

Figure 2.2 Principle of moire interferometry (undeforemed specimen)

Consider two grating lines, one of which is stationary on the specimen that will deform and then the other of which is the grating's reference line, to utilize the Moire method to measure deformation (Eindhoven et al., 2022). When the current is in a direction perpendicular to the scar, an increase in the moire fringes will result in a displacement of the scar bleach on the specimen part compared to the reference scar (Cubreli et al., 2021) . The scar field p of each Moire edge represents the displacement p, with the frequency of the scar determining the sensitivity to each displacement. The frequency increase is used to boost the sensitivity with each shift (Melin, 1995).

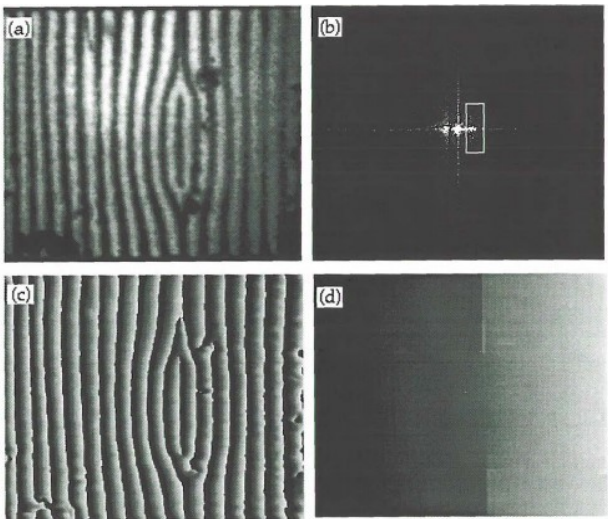

Figure 2.3 Analysis of moire fringe pattern on double edge specimen.

Shear interferometry is another method that is employed in the Moire method. Since the object beam will interfere with its replica and cause it to be deep within a tiny shear value, shear interferometry does not require a reference beam. The distribution of slow variations in the object's phase, as well as the interferogram's edges, contain information about the phase function's derivation. However, various Moire implementations of the edge technique in interferometry have been covered in the previous section, where it is an instrumental error rejection that switches from finite to infinite edge detection mode.

2.3 Digital Speckle Pattern Inteferometry

Digital speckle pattern interferometry, or DSPI, is an optical measurement technique that combines speckle pattern interferometry with electronic detection and processing (Andrés et al., 2013). It has been widely used in the investigation of a wide range of physical parameters in engineering structures, including displacement, vibrations, strains, and surface profiles.

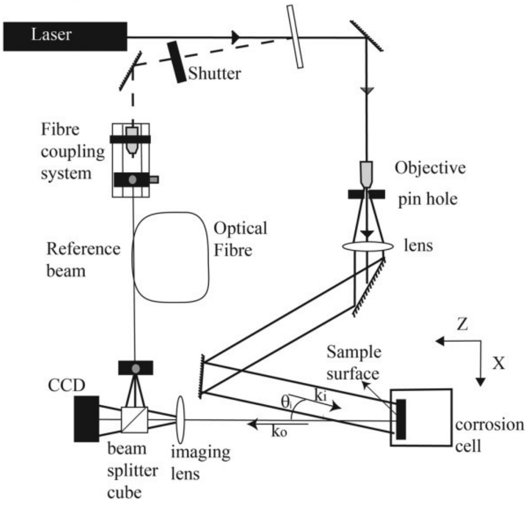

Figure 2.4 Optical Setup for the DSPI

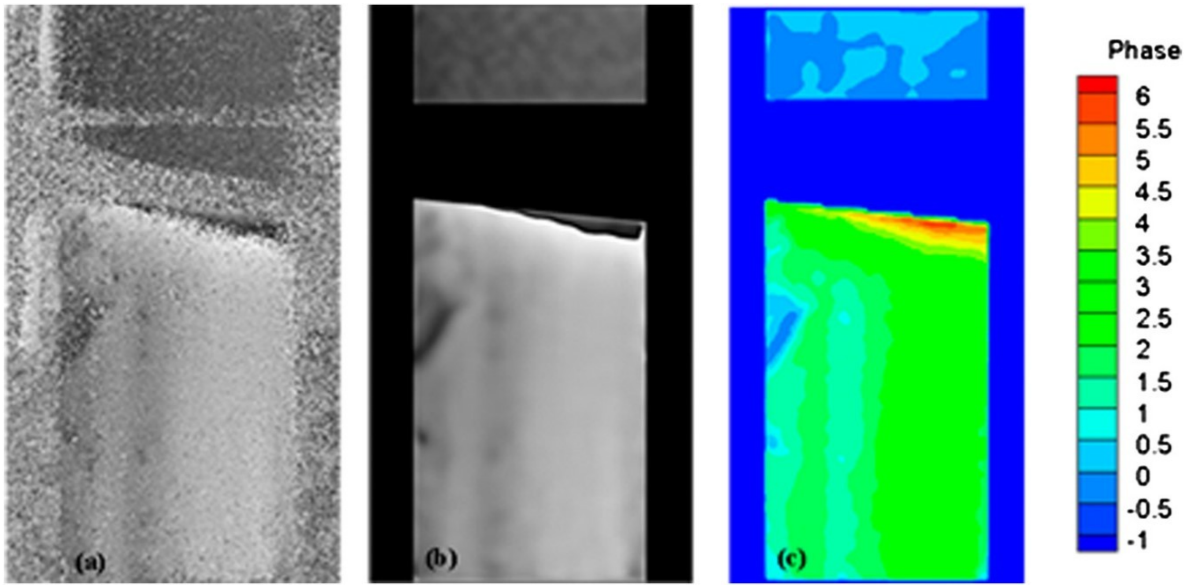

Figure 2.5 Phase map obtained by comparing then corrosion state after 180s

Beam expansion is created by two solid-state lasers with different wavelengths to illuminate the tested object. Scattered light reflects on the object's CCD plane as it passes through the shear device and into the picture (Andrés et al., 2013). A Michelson interferometer mirror that has been changed to tilt at a smaller angle, where the image captured on the CCD camera is emitted by shear, is responsible for the spatial frequency shift in the spatial frequency domain.

2.3.1 Static Speckle and Speckle Shear Fringe Analysis

There are two methods for static speckle and shear fringes: phase of differences technique (PDM) and difference of phases method (DPM) . Use single frames in the distorted state of the object instead of five altered frames in the un-deformed state for PDM. It employs a phase-shifted correlation fringe pattern, in which the phase-shifted intensity is subtracted from either the un-deformed or deformedstates, or vice versa(Cubreli et al., 2021) . The DPM, on the other hand, relied on phase correlation rather than speckle intensity correlation. The phase maps will be calculated individually for the deformed and un-deformed states utilizing phase shifting techniques for the DPM.

2.3.2 Quasi-Dynamic Speckle and Shear Fringe Analysis

The quasi-dynamic response of an item can be investigated on different loads, as well as the deformation and gradient, using the 'phase of differences' method(Hossack, 1998). Figures below demonstrate speckle correlation and speckle correlation patterns obtained from a dual function DSPI system at different times.

Figure 2.6 (a) (b) Speckle Correlation

2.4 Holographic Inteferometry

Three-dimensional images can be created using holographic technology. This holographic technology can be used in art as well as commercial applications such as souvenirs and credit cards (Cubreli et al., 2021) . As a result of the holographic ability to record and reconstruct light waves, a 3D image is obtained. It will compare the two light waves that emanate from the same object before and after distortion using holographic inteferometry. The two light waves will collide, causing an optical effect to occur on the fringe pattern, which will provide information about the object's deformation (Hossack, 1998).This complete field data is critical because it may be used in mechanical experiments to calculate deformation, stress, and strain for the visible region of a loaded item.

Digital holographic interferometry (DHI), which is regarded as one of the most precise. Holography, also known as wavefront reconstruction, use the recording and reproducing the amplitude and phase variations throughout a wavefront. When monochromatic light enters the eyes or any other optical device, the amplitude and phase of the fluctuation over the input aperture are the only data provided(Dhirubhai et al., 2015). As a result, the waveform will be holographically reconstructed to be equivalent to the original optic wave.

When compared to traditional optical interferometry approaches, the usage of a hologram provides a distinct benefit. Comparing holograms made of the same object under different conditions at different dates can reveal structural changes. The full object surface would be captured, allowing the displacement effects of the object to be seen in their entirety. The real-time hologram allows for immediate monitoring of minute changes in an object as it is stressed(Dhirubhai et al., 2015). The hologram of the object to be researched was overlaid on the actual object. When the object is subjected to stress conditions, any deformation in the surface will be visible as fringe interference patterns. The degree and direction of deformation are revealed in great detail by measuring these patterns(Brooks, 1969).

2.5 Finite Element Analysis(FEA)

Finite element analysis (FEA) is a method of simulating a part's or assembly's behaviour under specific circumstances in order to assess this using the finite element method (FEM) (Jagota et al., 2013). Engineers utilize FEA to help them model physical processes and so reduce the requirement for actual prototypes, while also allowing for component optimization as part of the project's design process (Analysis, 2018).

To comprehend and quantify the impacts of real-world conditions on a part or assembly, FEA employs mathematical models. These simulations will be carried out using specialized software that allows engineers to discover potential design flaws such as tension and weak points (Davila, 2020).

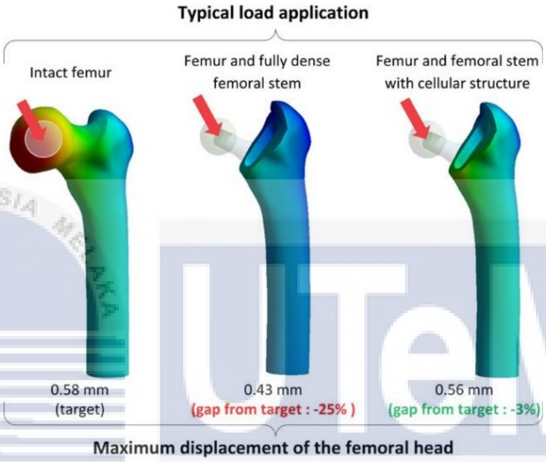

Figure 2.7 Analysis using the FEA

2.6 Result Digital Image Correlation On The Concrete Beams

The failure parameter can always be detected using the DIC by running it via software. Digital Image Correlation (DIC) is a vision-based technique that employs picture recognition and mapping technologies to properly measure 2D image variances(Mousa et al., 2021). With photos of the targeted system taken at different times, DIC can be used for routine or long-term observation. Images from various periods can be visually inspected with software, and deformations can be calculated from the data.

Time application techniques are less definable and exact than DIC. DIC also uses classic electronic imagery, which can be used with civil construction procedures to give precise mathematical assessments of components or systems in traditional outdoor settings (Ahmad & Fırıncıoğlu, 2020).Furthermore, because the targeted system's existing layer has appropriate photographic texture, no specialized lighting is required, and in some cases, DIC can function even without specific surface preparing.

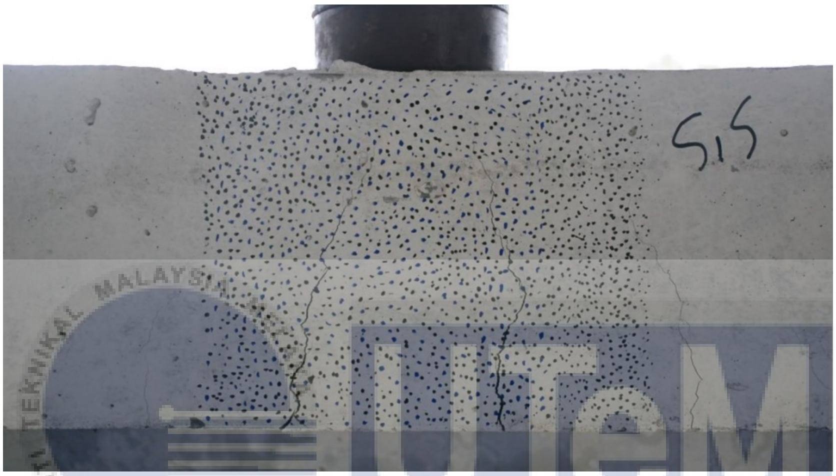

Figure 2.8 Crack on the beam before analysis

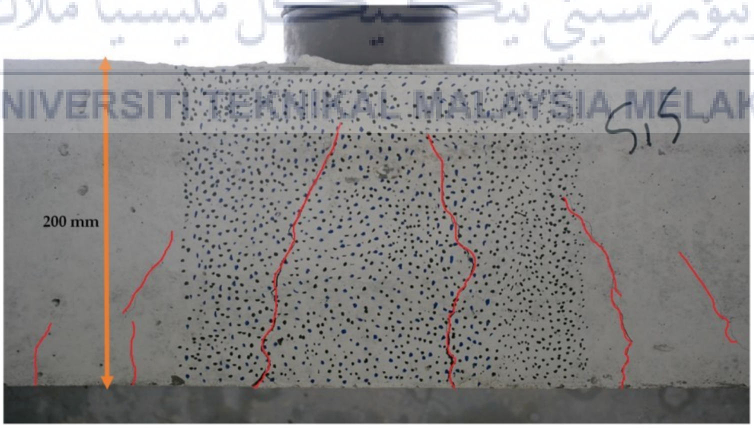

Figure 2.9 Crack on the beam before analysis

Figure 2.9 shows that using a marker pen to identify such cracks is possible, though it is a time-consuming and disorganized operation. Inside the speckled zone, a single photograph taken before cracking appeared and another taken after cracking appeared can be used to determine the overall actual quantity and quality of cracks (Mousa et al., 2021). This method has several advantages in effective detection that grow without causing touch. It also provides useful information regarding where fracture dispersion detectors can be attached, as well as exact crack calculations, even in cases when crack margins are poorly defined.

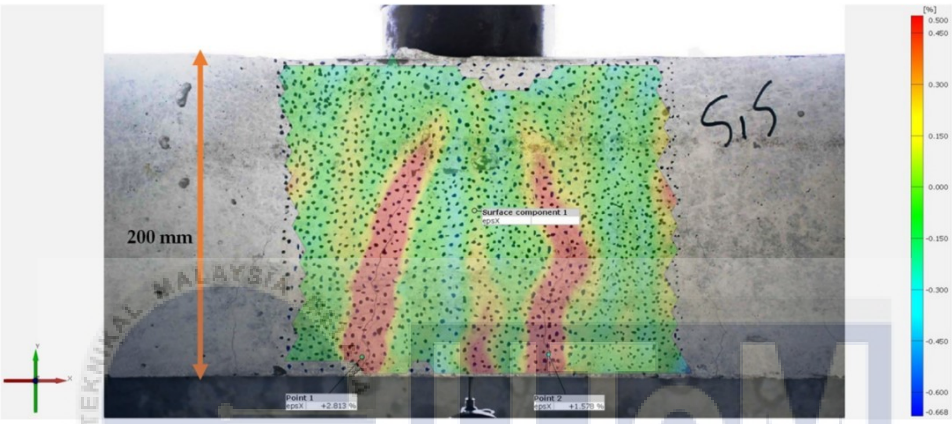

Figure 2.10 Analysis for the deformation

The contour and all the tensile values can be obtained by running it through the software. Cross-correlation as a method of assessing changes in data methods has been known for a long time and has been applied to electronically imaging since the 1970s (Ahmad & Fırıncıoğlu, 2020). Researchers in the 1980s inspired the first investigations, basis, and framework in DIC approaches in mechanics. Subset-based DIC approaches, such as 2D and 3D ideas, were established around this time and have not seen significant changes since then. A novel global finite element-based technique for the DIC correlation algorithm has been created as computer computing powers have improved.

2.7 Result On Structural Health Monitoring the Bridges Structure Using DIC

The use of low-cost, easily implemented, and sufficiently precise monitoring systems is a crucial approach to long-term civil infrastructure cost-effective management. These requirements are met by the Digital Image Correlation (DIC) (Ahmad & Fırıncıoğlu, 2020). Because of their enormous size, DIC sensors are an ideal alternative to traditional sensors for civil and structural monitoring because they allow assessments to be carried out without interfering with system functionality and can reach locations that are difficult to reach without the use of special machinery such as scaffolds and trucks(Mousa et al., 2021). Many researchers have realized the efficiency and applicability of vision-based and DIC approaches for diverse SHM applications over the last two decades. Bridges are the most studied civil engineering systems due to their strategic importance and security implications. The following is a current state-of-the-art review of the latest SHM application for multiple bridge infrastructures using the DIC approach.

2.7.1 Concretes Bridges

Arch, Reinforced Slab, Beam and Slab, Box Girder, Integral, and Cable-Stayed Bridges are the different types of concrete bridges. One of Lee and Shinozuka's first projects, in 2006, involved a concrete bridge with metal container girders, which will be discussed further under the bridge superstructure section.

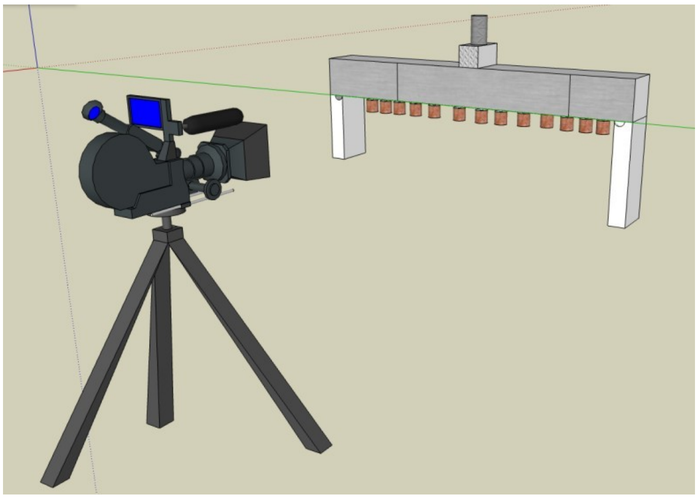

Figure 2.11 Setup on the Concretes bridges

In this experiment, a heavyweight was suspended from a bridge. Photographs of the girder surface before and after deformation were taken using a single electronic camera (Mousa et al., 2021). The results showed that the DIC-recorded deflections agreed with those reported with the Linear Variable Differential Transformer (LVDT), implying that the proposed technique could eliminate the influence of camera motion. created an innovative prototype pairing optimization technique up-sampled cross-correlation using Fourier transform to extract displacements in real-time from video images.

The findings revealed that increased imagery resolution of less than 1 mm could be achieved with ease by just changing the up-sampling value. The displacements observed by the single camera coincided with measured displacements acquired from the high-performance laser sensors, according to a field test conducted on a railway and pedestrian bridge (Eichhorn, 2019). The vision-based method has a number of advantages, including the ability to extract structural deflections from a single measurement at any position, as well as its ease of use and low cost.

2.7.2 Suspension Bridges

Another application for infrastructure, particularly cable-stayed bridges, was the monitoring of hanger cables. Ji et al. were among the first to propose using a combination of 2D- and 3D-DIC techniques to measure vibrations of cables holding a pedestrian bridge using optical sensors in 2008. The proposed strategy studied a series of photographs captured from a vibrating wire and inputted the intensity of optical variance of a targeted region of reference to determine the wire displacement using a single commercially available camera device with no camera calibration required prior to testing. The results of the experiments show that the method can accurately measure cable vibration and pipe motion. Furthermore, by obviating the need to append a target to the optical flow, this strategy enables for straightforward implementation.

2.7.3 Strain Measurement In Friction Stir Weld (FSW) Sample

Friction Stir welding is a solid-state welding technique for combining metals that involves plasticizing and consolidating materials along the bond line with the use of heat energy generated by localized friction forces. This welding procedure is used in a variety of aerospace applications, and it is frequently used to evaluate the welded zone for weld integrity. The material parameters of the weld samples, such as the Young's modulus and yield stresses, were also determined using the SPDIC tool's stress-strain graphs. Furthermore, the pseudo coloured strain contour maps highlighted the location of maximal strain, allowing fracture initiation in the sample to be predicted.

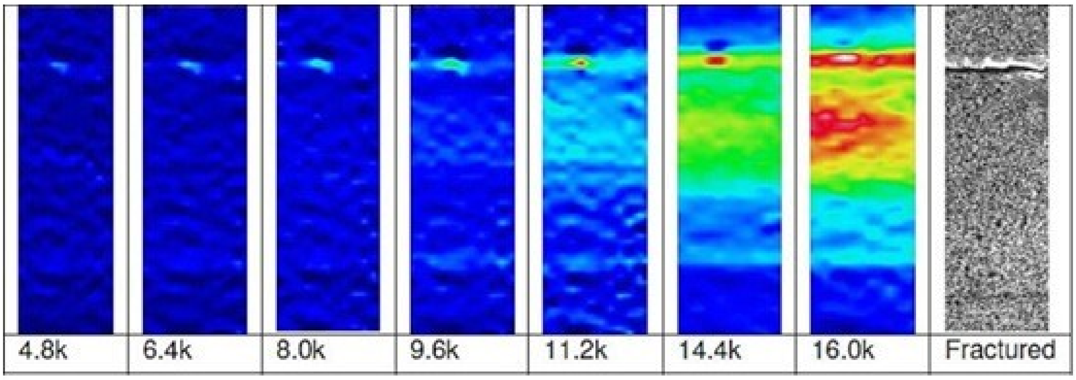

Figure 2.12 Sample of analysis on the structure

To be able analyse the data, some equipment need to be focus on it used. By using the best equipment, the result analysis of data will be great and easy to get.

2.8 CAMERA

Camera is used to capture images or record any video. However, to obtain the good result, the camera that need to be use d high speed camera. A high-speed camera is one that can capture moving images with exposures of less than 1/1,000 second and frame rates of more than 250 frames per second. Early elementary cameras used film to record high-speed events, but these were gradually replaced by entirely electronic devices that used either a charge-coupled device (CCD) or a CMOS active pixel sensor to record over 1,000 frames per second onto DRAM, which could then be replayed slowly to conduct research the motion for scientific inquiry of transient phenomena.

2.8.1 LaVision camera

For strain and deformation analysis, LaVision offers a broad array of cameras. We offer high-resolution and high-frame-rate cameras, relying on your requirements.

The Imager M-lite is a high sensitivity, high - definition USB 3 camera series, equipped with the newly developed CMOS sensors with improved image quality and low readout noise. Models with resolutions ranging from 2 to 16 million pixels are available.

Figure 2.13 Lavision Camera

2.8.2 Photron and Phantom cameras

The programme fully integrates the Photron and Phantom cameras, which have CMOS sensors with frame rates of several kHz and the best spatial resolution. LaVision's high-speed cameras, including all of its other cameras, are ready for use in time-resolved applications involving extremely high strain rates, such as impact or explosion.

Figure 2.14 Photron and Phantom camera

CHAPTER 3

METHODOLOGY

3.1 Introduction

The approach that was employed in this report will be discussed in this chapter. The methodology section of the report describes how the study was carried out, the research methodologies utilized, and the justifications for using those approaches. a discipline's set of methods, rules, and postulates such as a specific procedure or series of procedures exhibiting library research methodology. The problem is a massive rethinking of educational methods. It refers to the procedures or strategies used to find, select, process, and evaluate information about a certain subject. The methodology portion of a research article allows the reader to critically examine the study's overall validity and dependability.

3.2 Project Planning

The goal of project planning is to make sure the research or project runs smoothly. Flow charts can aid with the process of implementing each step one at a time for better order.

3.3 Proposed Methodology

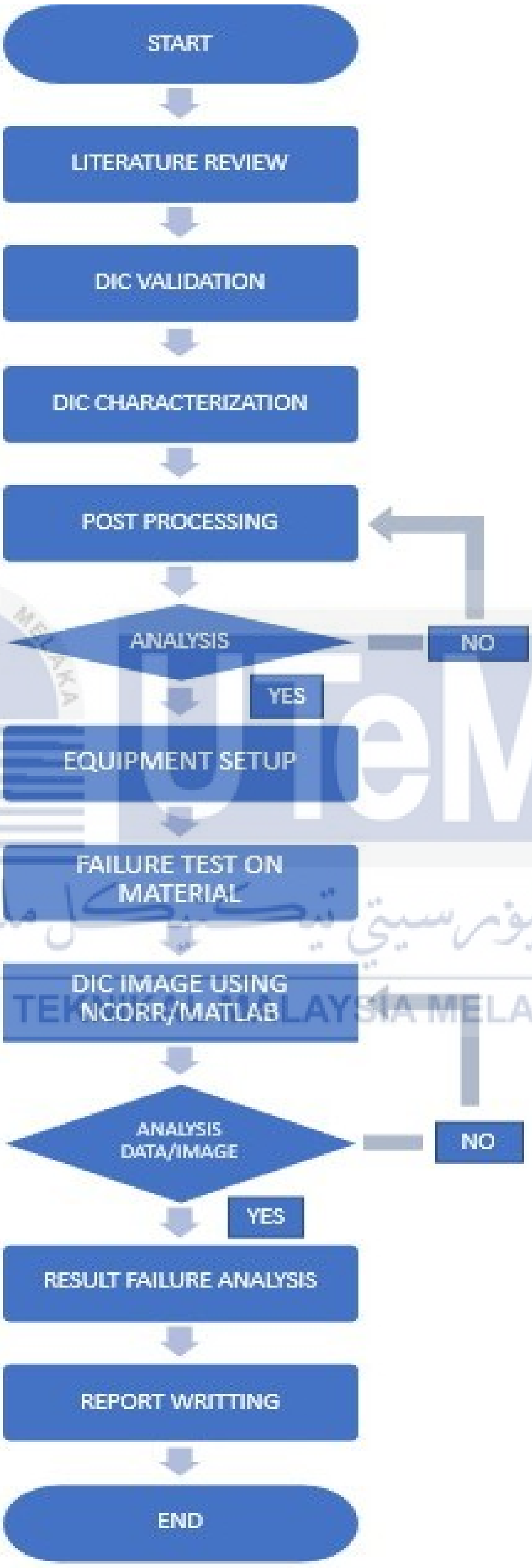

Figure 3.1 Flow Chart Process

3.3.1 DIC Validation

Validation is a one of the process that need to be run before proceed with the post processing and failure test on the real material. Each product or material must undergo the confirmation through series of the simple experiment step so that can be conclude either the material in the right term of it properties. This need to be run to ensure that all the specification of material and it experiment archive a good result.

3.3.2 DIC Characterization

Characterization for DIC is on DIC system for small biological specimens based on a high speed camera and original image correlation algorithm. Each material has it own characteristic to ensure it stability to use. Below are the some of the detail for the cable for crane.

Table 3.1 Specification detail for the steel wire ropes for crane

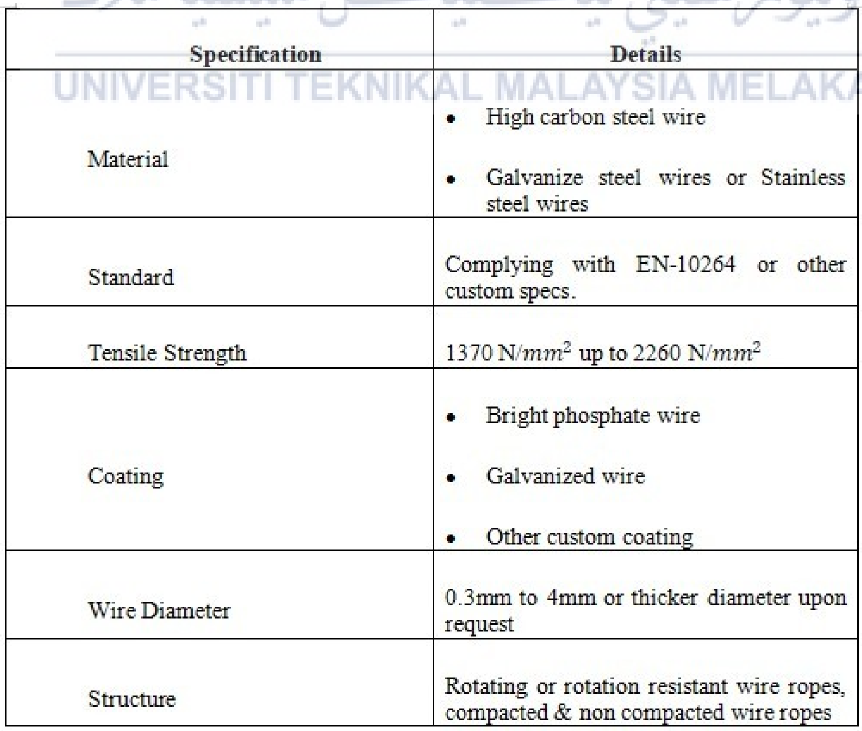

Specification	Details
Material	- High carbon steel wire - Galvanize steel wires or Stainless steel wires
Standard	Complying with EN-10264 or other custom specs.
Tensile Strength	1370 N/mm^2 up to 2260 N/mm^2
Coating	- Bright phosphate wire - Galvanized wire - Other custom coating
Wire Diameter	0.3mm to 4mm or thicker diameter upon request
Structure	Rotating or rotation resistant wire ropes, compacted & non compacted wire ropes

3.3.3 Post Processing

In this process will be discuss on how the analysis of DIC be made by using the Ncorr.

Below are the program flow that need to be follow :

1. Reference images need to be set.

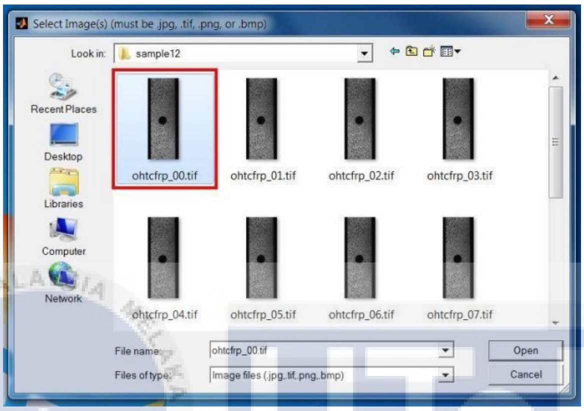

Look in: sample12

File name: ohtcfrp_00.tif

Files of type: Image files (.jpg,.tif,.png,.bmp)

Figure 3.2 Selection on reference image

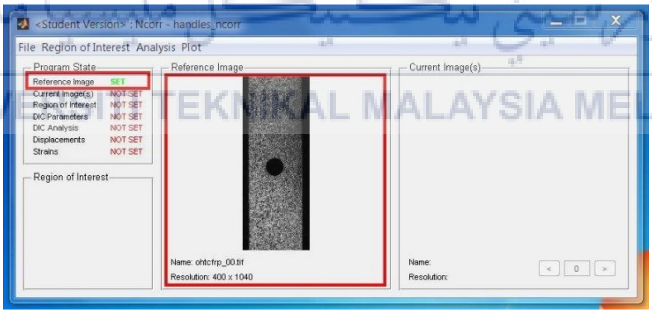

Program State	
Reference Image	SET
Current Image(s)	NOT SET
Region of Interest	NOT SET
DIC Parameters	NOT SET
DIC Analysis	NOT SET
Displacements	NOT SET
Strains	NOT SET

Name: ohtcfrp_00.tif

Resolution: 400 x 1040

Name:

Resolution:

Figure 3.3 Reference image been selected

2. Set the current image(s)

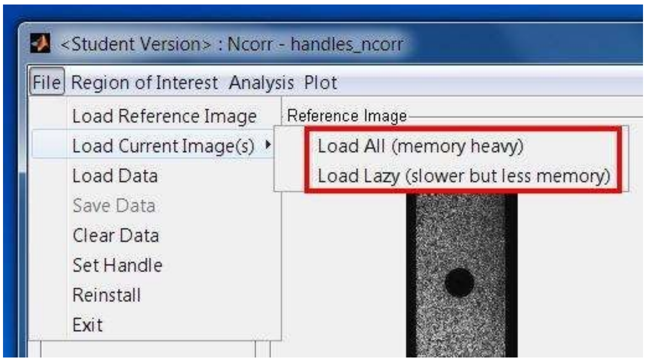

Figure 3.4 Choosing the Load Lazy for Current image

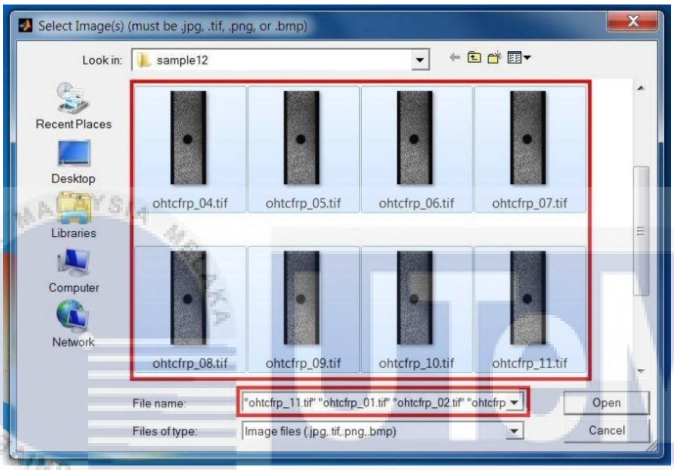

File name: "ohtcfrp_11.tif" "ohtcfrp_01.tif" "ohtcfrp_02.tif" "ohtcfrp

Files of type: Image files (.jpg,.tif,.png,.bmp)

Figure 3.5 Select current images

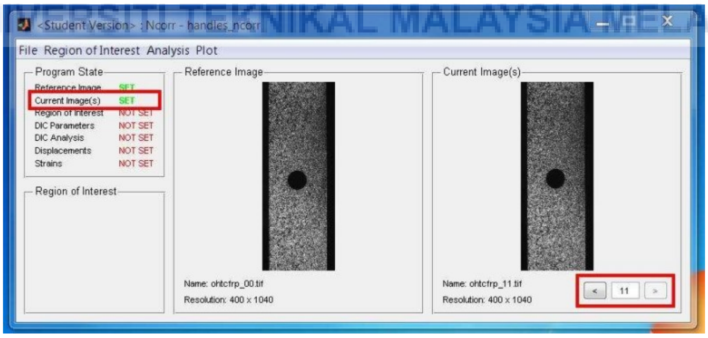

Program State	
Reference Image	SET
Current Image(s)	SET
Region of Interest	NOT SET
DIC Parameters	NOT SET
DIC Analysis	NOT SET
Displacements	NOT SET
Strains	NOT SET

Name: ohtcfrp_00.tif
Resolution: 400 x 1040

Name: ohtcfrp_11.tif
Resolution: 400 x 1040

Figure 3.6 Images been selected

3. Region of interest setting(ROI)

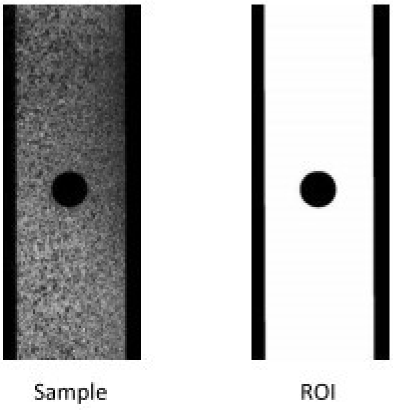

Figure 3.7 Different between ROI and sample

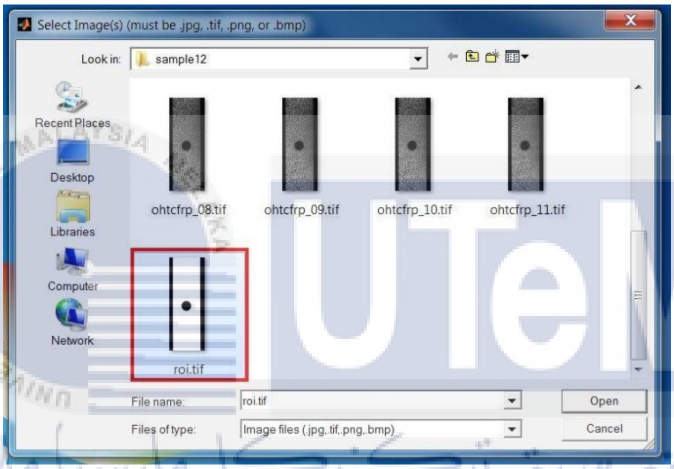

Select Image(s) (must be .jpg, .tif, .png, or .bmp)

Look in: sample12

File name: roi.tif

Files of type: Image files (.jpg,.tif,.png,.bmp)

Figure 3.8 ROI selection

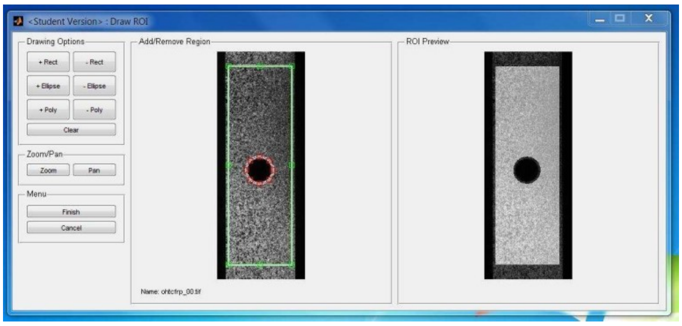

<Student Version> : Draw ROI

Name: ohtcfrp_00.tif

Figure 3.9 Drawing ROI

4. DIC parameter setting

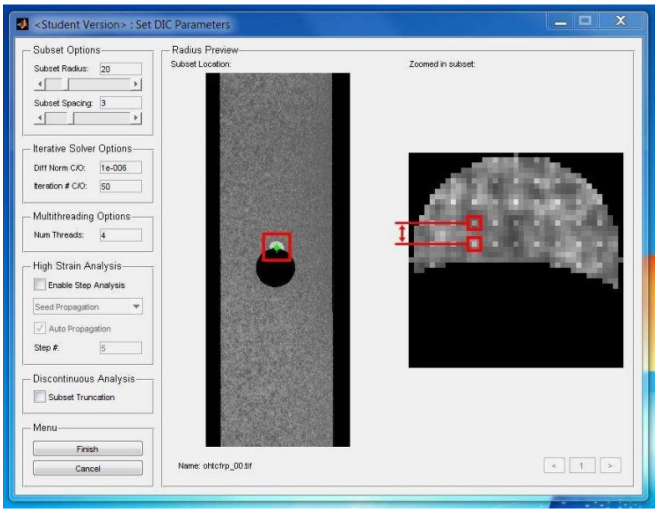

Subset Radius: 20

Subset Spacing: 3

Diff Norm C/O: 1e-006

Iteration # C/O: 50

Num Threads: 4

Step #: 5

Name: ohtcfrp_00.tif

Figure 3.10 Subset radius & subset spacing

5. DIC analysis

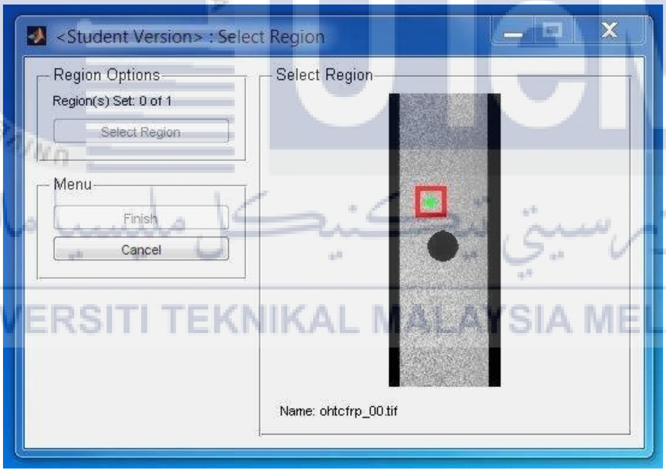

Region(s) Set: 0 of 1

Name: ohtcfrp_00.tif

Figure 3.11 Regions selection

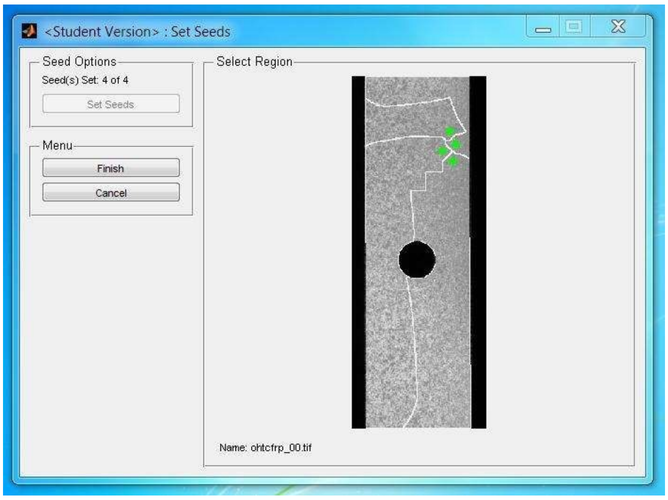

Seed(s) Set: 4 of 4

Name: ohtcfrp_00.tif

Figure 3.12 Wrong selection of seed place

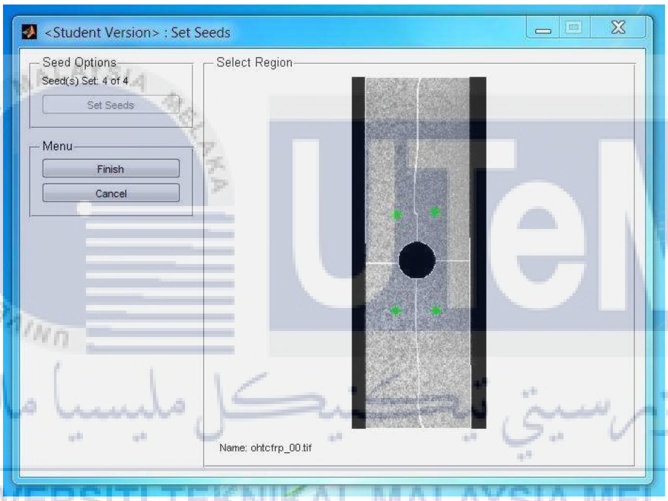

Seed(s) Set: 4 of 4

Name: ohtcfrp_00.tif

Figure 3.13 Right seed region

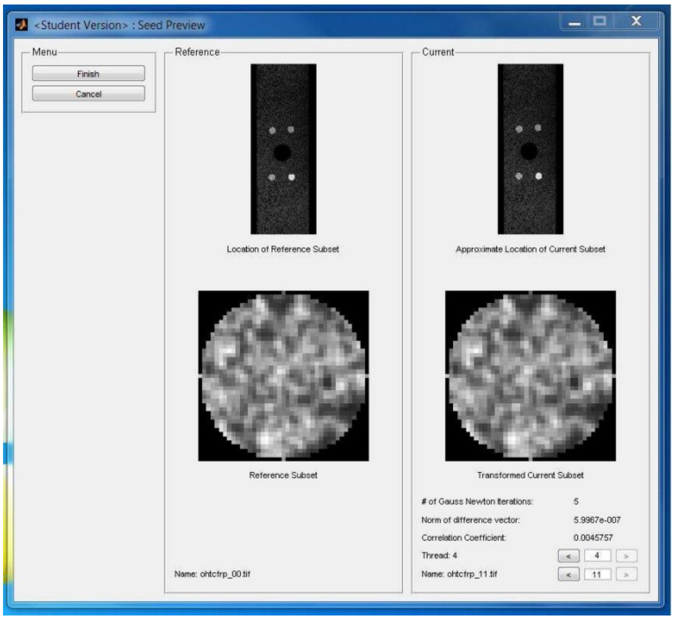

# of Gauss Newton Iterations: 5
Norm of difference vector: 5.9967e-007
Correlation Coefficient: 0.0045757
Thread: 4
Name: ohtcfrp_00.tif
Name: ohtcfrp_11.tif

Figure 3.14 Preview for seed region

6. Format displacement

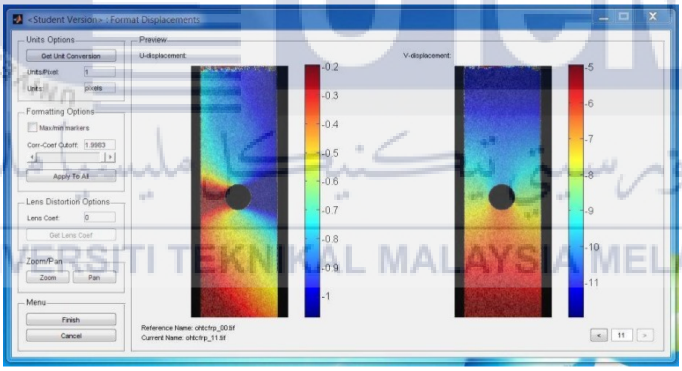

Units/Pixel: 1
Units: pixels
Corr-Coef Cutoff: 1.9983
Lens Coef: 0
Reference Name: ohtcfrp_00.tif
Current Name: ohtcfrp_11.tif

Figure 3.15 Format displacement

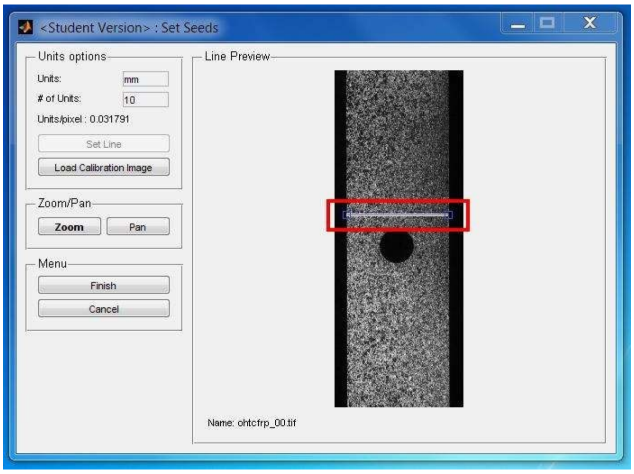

Units: mm

# of Units: 10

Units/pixel : 0.031791

Name: ohtcfrp_00.tif

Figure 3.16 Image calibration

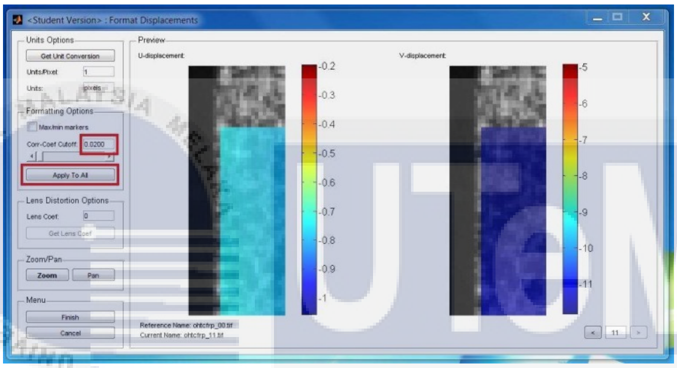

Units/Pixel: 1

Units: pixels

Corr-Coef Cutoff: 0.0200

Lens Coef: 0

Reference Name: ohtcfrp_00.tif

Current Name: ohtcfrp_11.tif

Figure 3.17 Unit and value setting

7. Calculate Strain

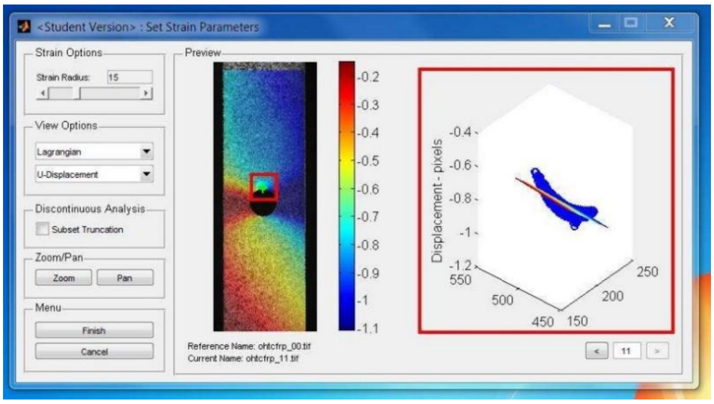

Strain Radius: 15

Lagrangian

U-Displacement

Reference Name: ohtcfrp_00.tif

Current Name: ohtcfrp_11.tif

Figure 3.18 Strain analysis

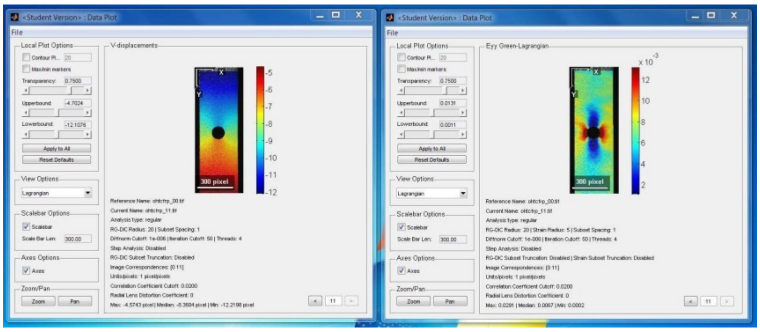

☐ Contour Pl... 20
☐ Max/min markers
Transparency: 0.7500
Upperbound: -4.7024
Lowerbound: -12.1076
Lagrangian
☑ Scalebar
Scale Bar Len: 300.00
☑ Axes

Reference Name: ohtcfrp_00.tif
Current Name: ohtcfrp_11.tif
Analysis type: regular
RG-DIC Radius: 20 | Subset Spacing: 1
Diffnorm Cutoff: 1e-006 | Iteration Cutoff: 50 | Threads: 4
Step Analysis: Disabled
RG-DIC Subset Truncation: Disabled
Image Correspondences: [0 11]
Units/pixels: 1 pixel/pixels
Correlation Coefficient Cutoff: 0.0200
Radial Lens Distortion Coefficient: 0
Max: -4.5743 pixel | Median: -8.3604 pixel | Min: -12.2198 pixel
< 11 >

☐ Contour Pl... 20
☐ Max/min markers
Transparency: 0.7500
Upperbound: 0.0131
Lowerbound: 0.0011
Lagrangian
☑ Scalebar
Scale Bar Len: 300.00
☑ Axes

Reference Name: ohtcfrp_00.tif
Current Name: ohtcfrp_11.tif
Analysis type: regular
RG-DIC Radius: 20 | Strain Radius: 5 | Subset Spacing: 1
Diffnorm Cutoff: 1e-006 | Iteration Cutoff: 50 | Threads: 4
Step Analysis: Disabled
RG-DIC Subset Truncation: Disabled | Strain Subset Truncation: Disabled
Image Correspondences: [0 11]
Units/pixels: 1 pixel/pixels
Correlation Coefficient Cutoff: 0.0200
Radial Lens Distortion Coefficient: 0
Max: 0.0291 | Median: 0.0067 | Min: 0.0002
< 11 >

Figure 3.19 Strain plotting

Figures below show the sample of loading flexural for the Ncorr or MatLab analysis.

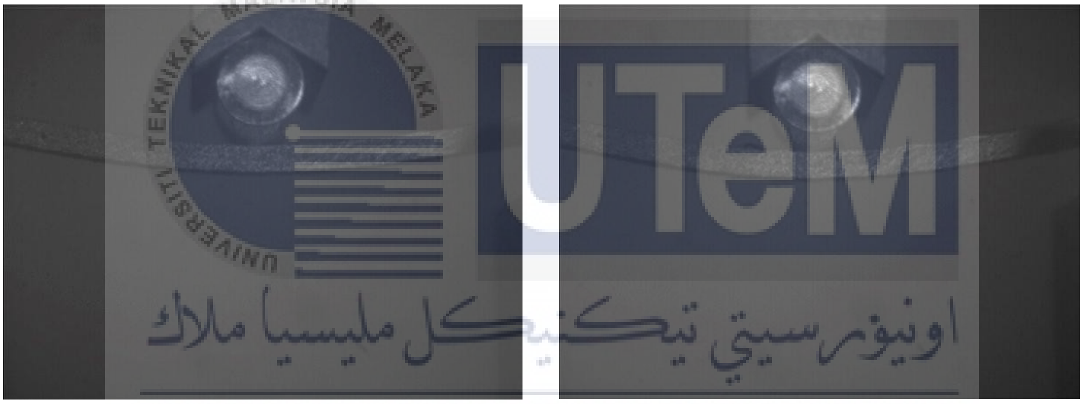

Figure 3.20 earlier image before failure

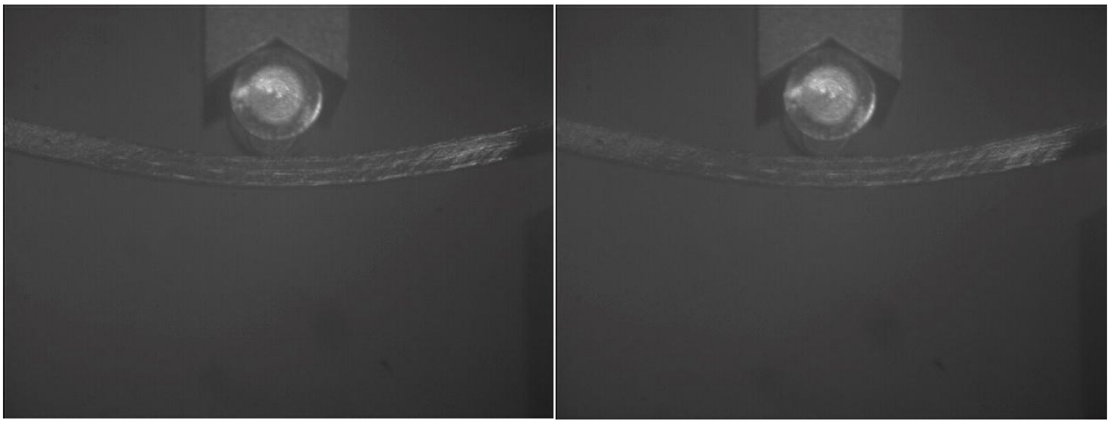

Figure 3.21 Image that almost failure

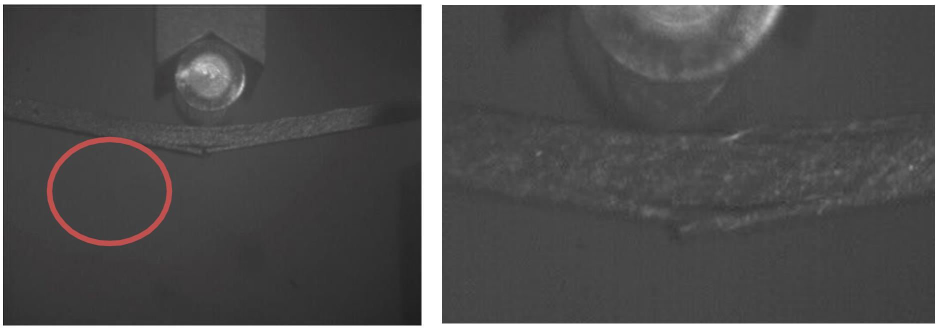

Figure 3.22 Specimen after failure

After undergo the analysis , the images will be display in the contour so that it will be easy to see the failure part either with the specification of deformation value.

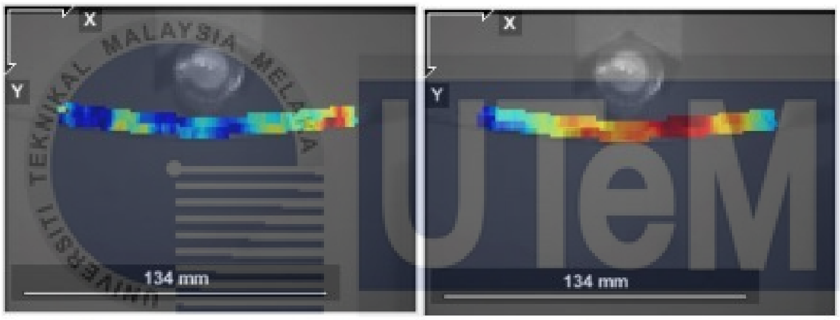

Figure 3.23 Analysis of deformation for the loading flexural

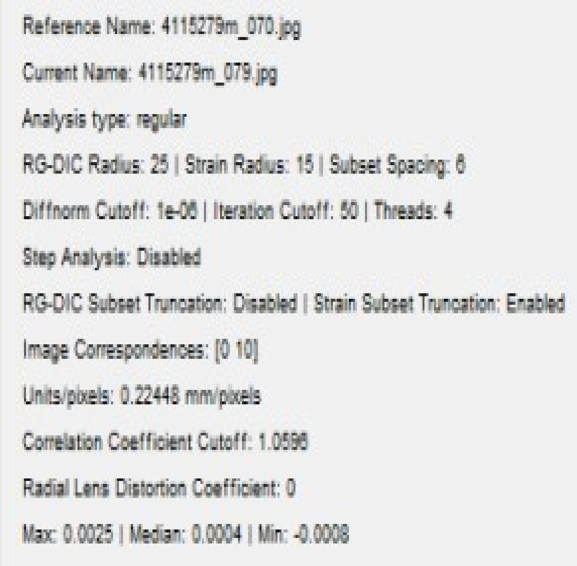

```
Reference Name: 4115279m_070.jpg

Current Name: 4115279m_079.jpg

Analysis type: regular

RG-DIC Radius: 25 | Strain Radius: 15 | Subset Spacing: 6

Diffnorm Cutoff: 1e-06 | Iteration Cutoff: 50 | Threads: 4

Step Analysis: Disabled

RG-DIC Subset Truncation: Disabled | Strain Subset Truncation: Enabled

Image Correspondences: [0 10]

Units/pixels: 0.22448 mm/pixels

Correlation Coefficient Cutoff: 1.0596

Radial Lens Distortion Coefficient: 0

Max: 0.0025 | Median: 0.0004 | Min: -0.0008
```

Figure 3.24 Data analysis for the loading flexural

3.3.4 Experimental Setup

Experimental setup is on how to manage the DIC from the taking images till get the analysis of the data for the correlation.

1. Principle

From the data obtain, the value of yield strength for the material or cable will be able to calculate by using the data .Stress relates to the forces operating on the component, whereas strain defines how the component deforms in reaction to the stress relative to its undefined condition. The following are the assumptions used in linear stress calculations:

$$\sigma = \frac{F}{A} \qquad [1]$$

and this presupposes...

stiffness * displacement = force

As a result, the component's reaction to stress is determined by both stiffness and geometry, and the material qualities have an immediate impact on this computation.

To determine how a component will react to stress, we must first determine the strain that the result will experience. Strain is attributed to the difference in the original item's size/shape and is computed as follows:

$$\varepsilon = \frac{\Delta l}{l} \qquad [2]$$

The connection between stress and strain is linear until it reaches the point of failure, which is referred to as UTS (ultimate tensile strength). Young's modulus (the elastic modulus) defines this linear relationship as follows:

modulus of elasticity = longitudinal stress / strain

$$y = \frac{\sigma}{\varepsilon} \qquad [3]$$

The slope of the graph displayed for the stress/strain relationship is determined by this relationship.

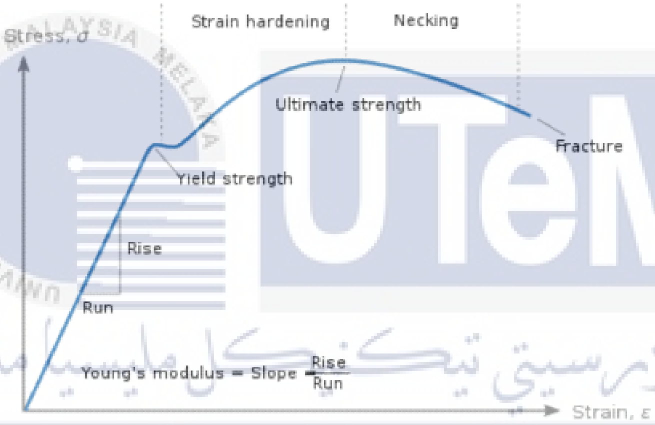

Figure 3.25 Stress Strain graph

2. Equipment

a) CABLE

This cable will go through a dic procedure, in which our camera holding the weight will record the cable's durability. Depending on everyday use, each material has a different level of durability. Using existing tools, the cable video recordings will be transformed into images for study.

Figure 3.26 Cable and Crane that will be used for DIC

b) SOFTWARE

To run the DIC analysis, it will use the MATLAB R2022a software which has already synchronize with the digital image correlation.

Figure 3.27 Matlab R2022a

3.4 Limitation of Proposed Methodology

Limitation is a some difficulty that encounter during the whole process of project. In this task, placing the right subset and choose the right subset size is one of the difficulty. By choosing the right size and placing, the problem that the worst region of the surface pattern will be influences the performance of DIC across the entire image. To avoid the limitation, a Dynamic subset selection(DSS) algorithm is proposed to optimize the subset size for each of the point in an image before optimizing the correlation parameters.

CHAPTER 4

RESULTS AND DISCUSSION

4.1 Introduction

This chapter presents the results and analysis on the cable including the validation on the brass displacement. Then, the Matlab software are used with triangle equations to establish a distance for brass to differentiate the value of real image and Matlab value. Case studies are performed to validate the applicability of the proposed system with real data.

4.2 Results and Analysis

4.2.1 Strain Analysis

Table 4.1 Value for the Matlab Ncorr Settings

Subset radius	43
Subset spacing	3
Number of threads	2
Seed	2

Radius spacing	20

Table 4.2 Analysis Strain

U AND V	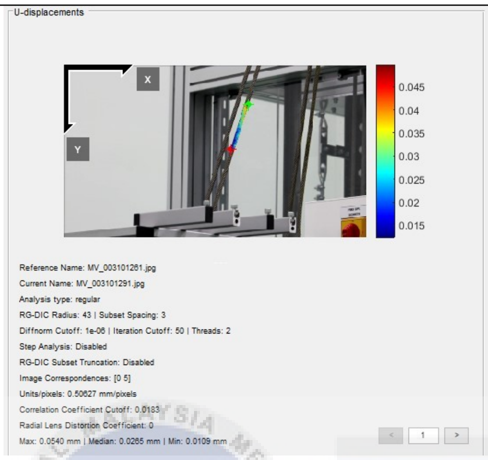 Reference Name: MV_003101261.jpg Current Name: MV_003101291.jpg Analysis type: regular RG-DIC Radius: 43 | Subset Spacing: 3 Diffnorm Cutoff: 1e-06 | Iteration Cutoff: 50 | Threads: 2 Step Analysis: Disabled RG-DIC Subset Truncation: Disabled Image Correspondences: [0 5] Units/pixels: 0.50627 mm/pixels Correlation Coefficient Cutoff: 0.0183 Radial Lens Distortion Coefficient: 0 Max: 0.0540 mm | Median: 0.0265 mm | Min: 0.0109 mm 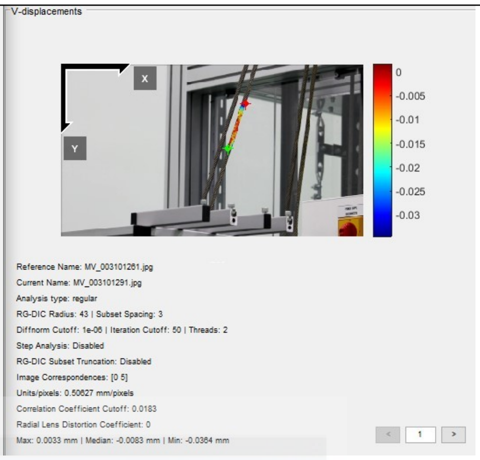 Reference Name: MV_003101261.jpg Current Name: MV_003101291.jpg Analysis type: regular RG-DIC Radius: 43 | Subset Spacing: 3 Diffnorm Cutoff: 1e-06 | Iteration Cutoff: 50 | Threads: 2 Step Analysis: Disabled RG-DIC Subset Truncation: Disabled Image Correspondences: [0 5] Units/pixels: 0.50627 mm/pixels Correlation Coefficient Cutoff: 0.0183 Radial Lens Distortion Coefficient: 0 Max: 0.0033 mm | Median: -0.0083 mm | Min: -0.0364 mm 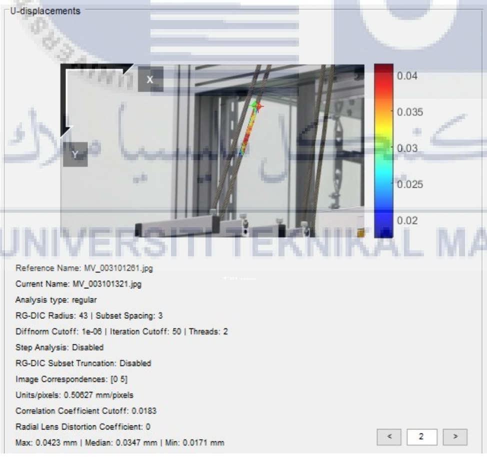 Reference Name: MV_003101261.jpg Current Name: MV_003101321.jpg Analysis type: regular RG-DIC Radius: 43 | Subset Spacing: 3 Diffnorm Cutoff: 1e-06 | Iteration Cutoff: 50 | Threads: 2 Step Analysis: Disabled RG-DIC Subset Truncation: Disabled Image Correspondences: [0 5] Units/pixels: 0.50627 mm/pixels Correlation Coefficient Cutoff: 0.0183 Radial Lens Distortion Coefficient: 0 Max: 0.0423 mm | Median: 0.0347 mm | Min: 0.0171 mm 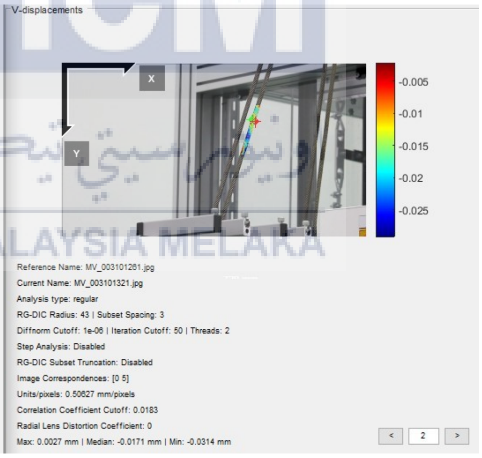 Reference Name: MV_003101261.jpg Current Name: MV_003101321.jpg Analysis type: regular RG-DIC Radius: 43 | Subset Spacing: 3 Diffnorm Cutoff: 1e-06 | Iteration Cutoff: 50 | Threads: 2 Step Analysis: Disabled RG-DIC Subset Truncation: Disabled Image Correspondences: [0 5] Units/pixels: 0.50627 mm/pixels Correlation Coefficient Cutoff: 0.0183 Radial Lens Distortion Coefficient: 0 Max: 0.0027 mm | Median: -0.0171 mm | Min: -0.0314 mm

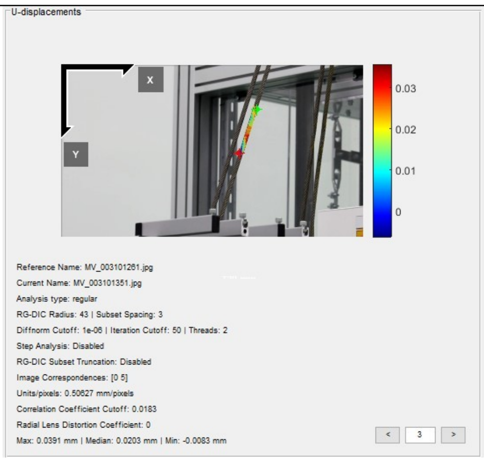

Reference Name: MV_003101261.jpg
Current Name: MV_003101351.jpg
Analysis type: regular
RG-DIC Radius: 43 | Subset Spacing: 3
Diffnorm Cutoff: 1e-06 | Iteration Cutoff: 50 | Threads: 2
Step Analysis: Disabled
RG-DIC Subset Truncation: Disabled
Image Correspondences: [0 5]
Units/pixels: 0.50627 mm/pixels
Correlation Coefficient Cutoff: 0.0183
Radial Lens Distortion Coefficient: 0
Max: 0.0391 mm | Median: 0.0203 mm | Min: -0.0083 mm

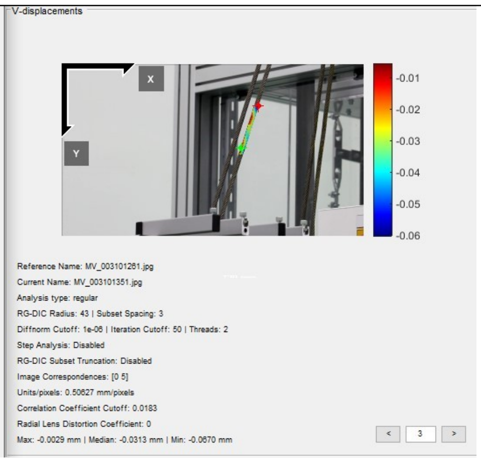

Reference Name: MV_003101261.jpg
Current Name: MV_003101351.jpg
Analysis type: regular
RG-DIC Radius: 43 | Subset Spacing: 3
Diffnorm Cutoff: 1e-06 | Iteration Cutoff: 50 | Threads: 2
Step Analysis: Disabled
RG-DIC Subset Truncation: Disabled
Image Correspondences: [0 5]
Units/pixels: 0.50627 mm/pixels
Correlation Coefficient Cutoff: 0.0183
Radial Lens Distortion Coefficient: 0
Max: -0.0029 mm | Median: -0.0313 mm | Min: -0.0670 mm

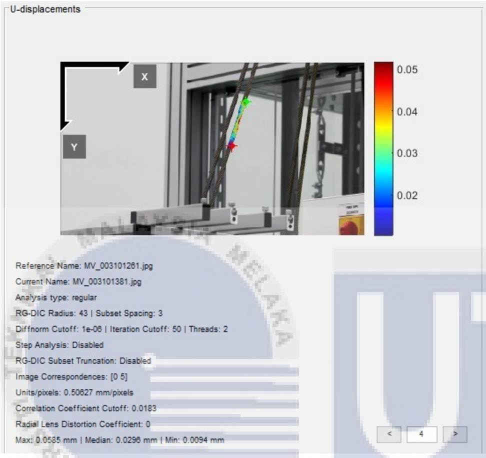

Reference Name: MV_003101261.jpg
Current Name: MV_003101381.jpg
Analysis type: regular
RG-DIC Radius: 43 | Subset Spacing: 3
Diffnorm Cutoff: 1e-06 | Iteration Cutoff: 50 | Threads: 2
Step Analysis: Disabled
RG-DIC Subset Truncation: Disabled
Image Correspondences: [0 5]
Units/pixels: 0.50627 mm/pixels
Correlation Coefficient Cutoff: 0.0183
Radial Lens Distortion Coefficient: 0
Max: 0.0585 mm | Median: 0.0296 mm | Min: 0.0094 mm

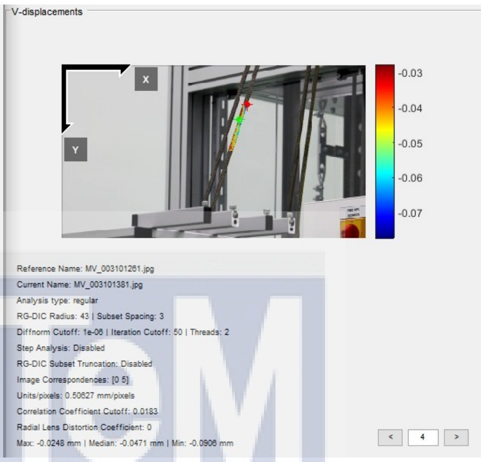

Reference Name: MV_003101261.jpg
Current Name: MV_003101381.jpg
Analysis type: regular
RG-DIC Radius: 43 | Subset Spacing: 3
Diffnorm Cutoff: 1e-06 | Iteration Cutoff: 50 | Threads: 2
Step Analysis: Disabled
RG-DIC Subset Truncation: Disabled
Image Correspondences: [0 5]
Units/pixels: 0.50627 mm/pixels
Correlation Coefficient Cutoff: 0.0183
Radial Lens Distortion Coefficient: 0
Max: -0.0248 mm | Median: -0.0471 mm | Min: -0.0906 mm

Reference Name: MV_003101261.jpg
Current Name: MV_003101411.jpg
Analysis type: regular
RG-DIC Radius: 43 | Subset Spacing: 3
Diffnorm Cutoff: 1e-06 | Iteration Cutoff: 50 | Threads: 2
Step Analysis: Disabled
RG-DIC Subset Truncation: Disabled
Image Correspondences: [0 5]
Units/pixels: 0.50627 mm/pixels
Correlation Coefficient Cutoff: 0.0183
Radial Lens Distortion Coefficient: 0
Max: 0.0292 mm | Median: 0.0055 mm | Min: -0.0221 mm

Reference Name: MV_003101261.jpg
Current Name: MV_003101411.jpg
Analysis type: regular
RG-DIC Radius: 43 | Subset Spacing: 3
Diffnorm Cutoff: 1e-06 | Iteration Cutoff: 50 | Threads: 2
Step Analysis: Disabled
RG-DIC Subset Truncation: Disabled
Image Correspondences: [0 5]
Units/pixels: 0.50627 mm/pixels
Correlation Coefficient Cutoff: 0.0183
Radial Lens Distortion Coefficient: 0
Max: -0.0171 mm | Median: -0.0618 mm | Min: -0.0989 mm

Exx and **Eyy**	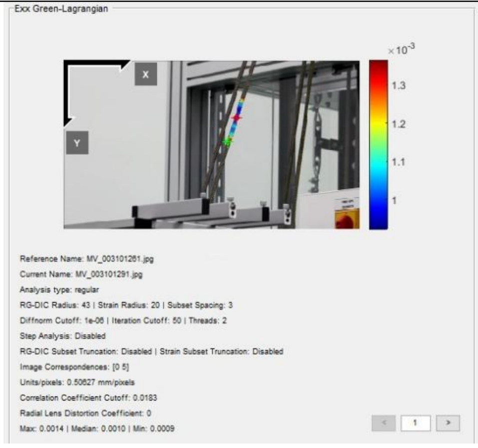 Reference Name: MV_003101261.jpg Current Name: MV_003101291.jpg Analysis type: regular RG-DIC Radius: 43 | Strain Radius: 20 | Subset Spacing: 3 Diffnorm Cutoff: 1e-06 | Iteration Cutoff: 50 | Threads: 2 Step Analysis: Disabled RG-DIC Subset Truncation: Disabled | Strain Subset Truncation: Disabled Image Correspondences: [0 5] Units/pixels: 0.50627 mm/pixels Correlation Coefficient Cutoff: 0.0183 Radial Lens Distortion Coefficient: 0 Max: 0.0014 | Median: 0.0010 | Min: 0.0009  Reference Name: MV_003101261.jpg Current Name: MV_003101291.jpg Analysis type: regular RG-DIC Radius: 43 | Strain Radius: 20 | Subset Spacing: 3 Diffnorm Cutoff: 1e-06 | Iteration Cutoff: 50 | Threads: 2 Step Analysis: Disabled RG-DIC Subset Truncation: Disabled | Strain Subset Truncation: Disabled Image Correspondences: [0 5] Units/pixels: 0.50627 mm/pixels Correlation Coefficient Cutoff: 0.0183 Radial Lens Distortion Coefficient: 0 Max: 0.0007 | Median: 0.0000 | Min: -0.0005 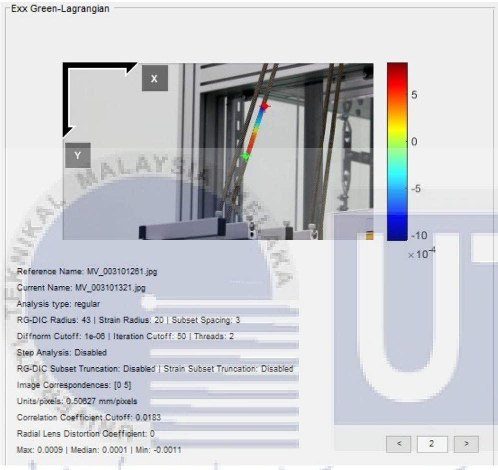 Reference Name: MV_003101261.jpg Current Name: MV_003101321.jpg Analysis type: regular RG-DIC Radius: 43 | Strain Radius: 20 | Subset Spacing: 3 Diffnorm Cutoff: 1e-06 | Iteration Cutoff: 50 | Threads: 2 Step Analysis: Disabled RG-DIC Subset Truncation: Disabled | Strain Subset Truncation: Disabled Image Correspondences: [0 5] Units/pixels: 0.50627 mm/pixels Correlation Coefficient Cutoff: 0.0183 Radial Lens Distortion Coefficient: 0 Max: 0.0009 | Median: 0.0001 | Min: -0.0011 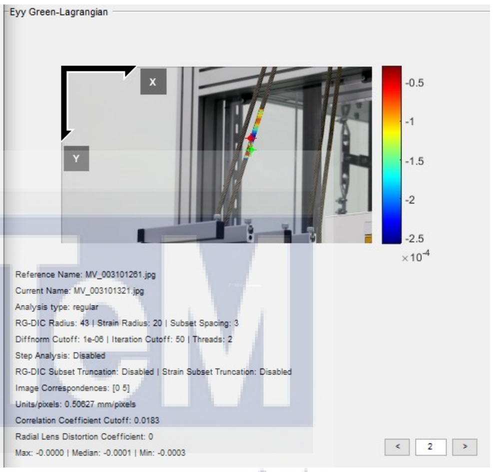 Reference Name: MV_003101261.jpg Current Name: MV_003101321.jpg Analysis type: regular RG-DIC Radius: 43 | Strain Radius: 20 | Subset Spacing: 3 Diffnorm Cutoff: 1e-06 | Iteration Cutoff: 50 | Threads: 2 Step Analysis: Disabled RG-DIC Subset Truncation: Disabled | Strain Subset Truncation: Disabled Image Correspondences: [0 5] Units/pixels: 0.50627 mm/pixels Correlation Coefficient Cutoff: 0.0183 Radial Lens Distortion Coefficient: 0 Max: -0.0000 | Median: -0.0001 | Min: -0.0003 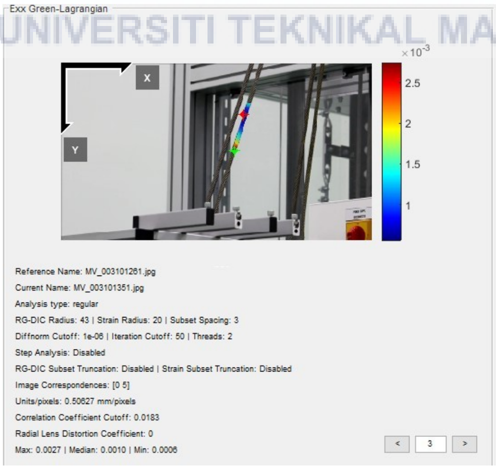 Reference Name: MV_003101261.jpg Current Name: MV_003101351.jpg Analysis type: regular RG-DIC Radius: 43 | Strain Radius: 20 | Subset Spacing: 3 Diffnorm Cutoff: 1e-06 | Iteration Cutoff: 50 | Threads: 2 Step Analysis: Disabled RG-DIC Subset Truncation: Disabled | Strain Subset Truncation: Disabled Image Correspondences: [0 5] Units/pixels: 0.50627 mm/pixels Correlation Coefficient Cutoff: 0.0183 Radial Lens Distortion Coefficient: 0 Max: 0.0027 | Median: 0.0010 | Min: 0.0006 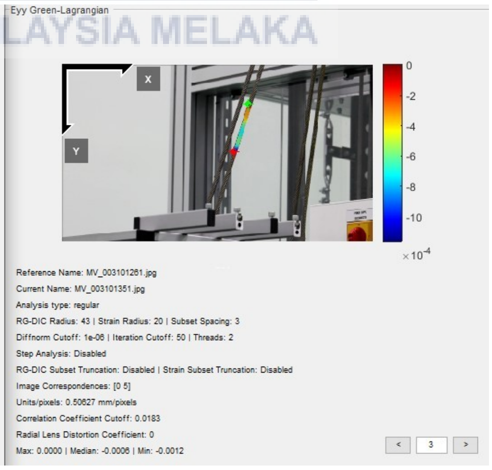 Reference Name: MV_003101261.jpg Current Name: MV_003101351.jpg Analysis type: regular RG-DIC Radius: 43 | Strain Radius: 20 | Subset Spacing: 3 Diffnorm Cutoff: 1e-06 | Iteration Cutoff: 50 | Threads: 2 Step Analysis: Disabled RG-DIC Subset Truncation: Disabled | Strain Subset Truncation: Disabled Image Correspondences: [0 5] Units/pixels: 0.50627 mm/pixels Correlation Coefficient Cutoff: 0.0183 Radial Lens Distortion Coefficient: 0 Max: 0.0000 | Median: -0.0006 | Min: -0.0012

	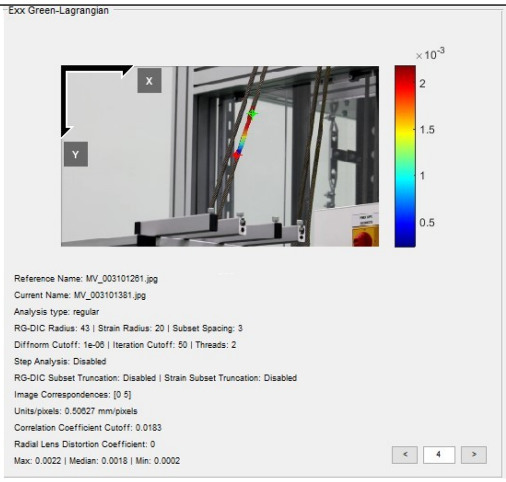 Reference Name: MV_003101261.jpg Current Name: MV_003101381.jpg Analysis type: regular RG-DIC Radius: 43 | Strain Radius: 20 | Subset Spacing: 3 Diffnorm Cutoff: 1e-06 | Iteration Cutoff: 50 | Threads: 2 Step Analysis: Disabled RG-DIC Subset Truncation: Disabled | Strain Subset Truncation: Disabled Image Correspondences: [0 5] Units/pixels: 0.50627 mm/pixels Correlation Coefficient Cutoff: 0.0183 Radial Lens Distortion Coefficient: 0 Max: 0.0022 | Median: 0.0018 | Min: 0.0002 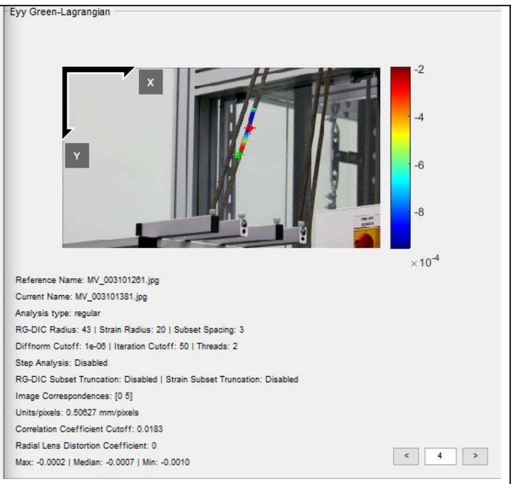 Reference Name: MV_003101261.jpg Current Name: MV_003101381.jpg Analysis type: regular RG-DIC Radius: 43 | Strain Radius: 20 | Subset Spacing: 3 Diffnorm Cutoff: 1e-06 | Iteration Cutoff: 50 | Threads: 2 Step Analysis: Disabled RG-DIC Subset Truncation: Disabled | Strain Subset Truncation: Disabled Image Correspondences: [0 5] Units/pixels: 0.50627 mm/pixels Correlation Coefficient Cutoff: 0.0183 Radial Lens Distortion Coefficient: 0 Max: -0.0002 | Median: -0.0007 | Min: -0.0010 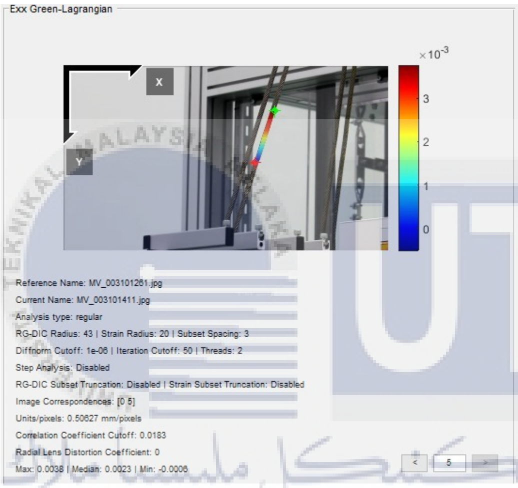 Reference Name: MV_003101261.jpg Current Name: MV_003101411.jpg Analysis type: regular RG-DIC Radius: 43 | Strain Radius: 20 | Subset Spacing: 3 Diffnorm Cutoff: 1e-06 | Iteration Cutoff: 50 | Threads: 2 Step Analysis: Disabled RG-DIC Subset Truncation: Disabled | Strain Subset Truncation: Disabled Image Correspondences: [0 5] Units/pixels: 0.50627 mm/pixels Correlation Coefficient Cutoff: 0.0183 Radial Lens Distortion Coefficient: 0 Max: 0.0038 | Median: 0.0023 | Min: -0.0006 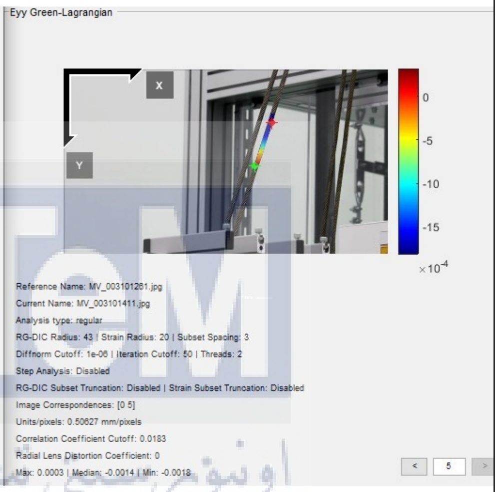 Reference Name: MV_003101261.jpg Current Name: MV_003101411.jpg Analysis type: regular RG-DIC Radius: 43 | Strain Radius: 20 | Subset Spacing: 3 Diffnorm Cutoff: 1e-06 | Iteration Cutoff: 50 | Threads: 2 Step Analysis: Disabled RG-DIC Subset Truncation: Disabled | Strain Subset Truncation: Disabled Image Correspondences: [0 5] Units/pixels: 0.50627 mm/pixels Correlation Coefficient Cutoff: 0.0183 Radial Lens Distortion Coefficient: 0 Max: 0.0003 | Median: -0.0014 | Min: -0.0018
Exy	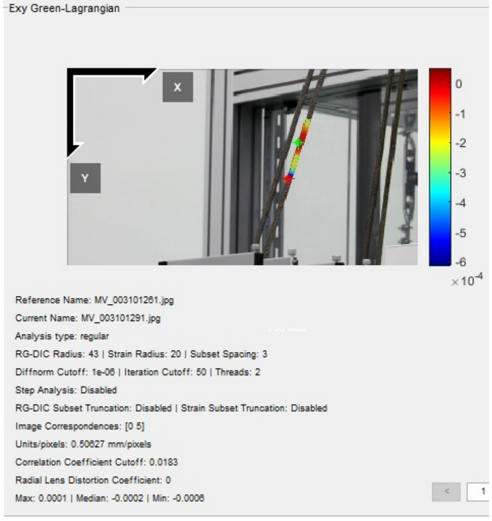 Reference Name: MV_003101261.jpg Current Name: MV_003101291.jpg Analysis type: regular RG-DIC Radius: 43 | Strain Radius: 20 | Subset Spacing: 3 Diffnorm Cutoff: 1e-06 | Iteration Cutoff: 50 | Threads: 2 Step Analysis: Disabled RG-DIC Subset Truncation: Disabled | Strain Subset Truncation: Disabled Image Correspondences: [0 5] Units/pixels: 0.50627 mm/pixels Correlation Coefficient Cutoff: 0.0183 Radial Lens Distortion Coefficient: 0 Max: 0.0001 | Median: -0.0002 | Min: -0.0006 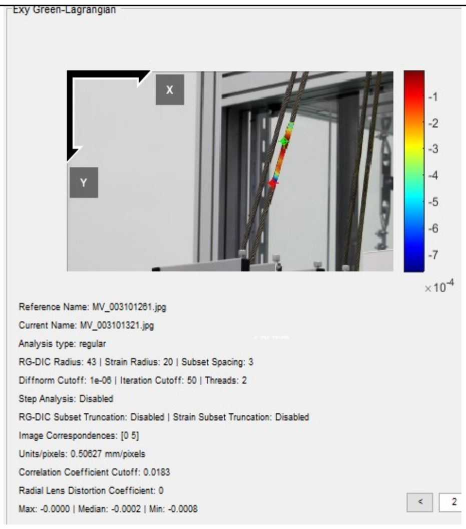 Reference Name: MV_003101261.jpg Current Name: MV_003101321.jpg Analysis type: regular RG-DIC Radius: 43 | Strain Radius: 20 | Subset Spacing: 3 Diffnorm Cutoff: 1e-06 | Iteration Cutoff: 50 | Threads: 2 Step Analysis: Disabled RG-DIC Subset Truncation: Disabled | Strain Subset Truncation: Disabled Image Correspondences: [0 5] Units/pixels: 0.50627 mm/pixels Correlation Coefficient Cutoff: 0.0183 Radial Lens Distortion Coefficient: 0 Max: -0.0000 | Median: -0.0002 | Min: -0.0008

	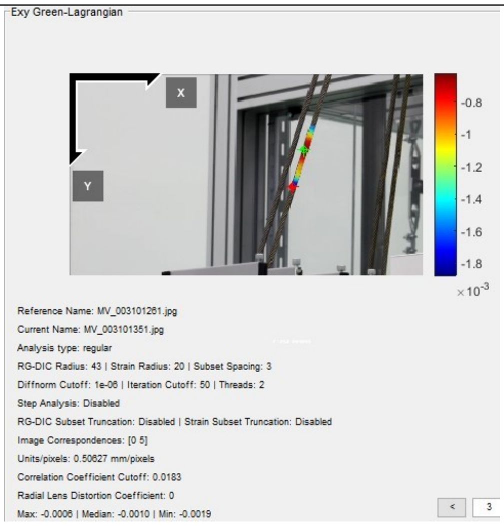 Reference Name: MV_003101261.jpg Current Name: MV_003101351.jpg Analysis type: regular RG-DIC Radius: 43 | Strain Radius: 20 | Subset Spacing: 3 Diffnorm Cutoff: 1e-06 | Iteration Cutoff: 50 | Threads: 2 Step Analysis: Disabled RG-DIC Subset Truncation: Disabled | Strain Subset Truncation: Disabled Image Correspondences: [0 5] Units/pixels: 0.50627 mm/pixels Correlation Coefficient Cutoff: 0.0183 Radial Lens Distortion Coefficient: 0 Max: -0.0006 | Median: -0.0010 | Min: -0.0019 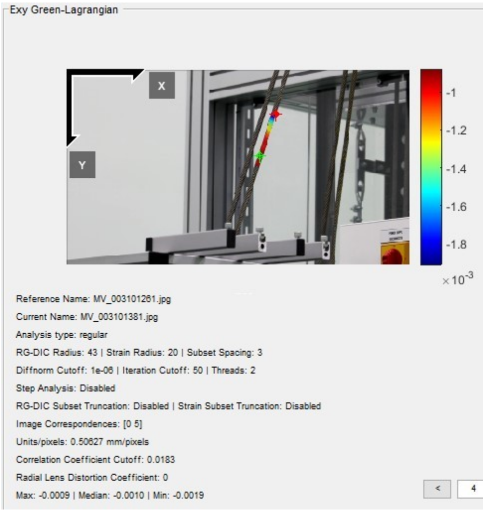 Reference Name: MV_003101261.jpg Current Name: MV_003101381.jpg Analysis type: regular RG-DIC Radius: 43 | Strain Radius: 20 | Subset Spacing: 3 Diffnorm Cutoff: 1e-06 | Iteration Cutoff: 50 | Threads: 2 Step Analysis: Disabled RG-DIC Subset Truncation: Disabled | Strain Subset Truncation: Disabled Image Correspondences: [0 5] Units/pixels: 0.50627 mm/pixels Correlation Coefficient Cutoff: 0.0183 Radial Lens Distortion Coefficient: 0 Max: -0.0009 | Median: -0.0010 | Min: -0.0019 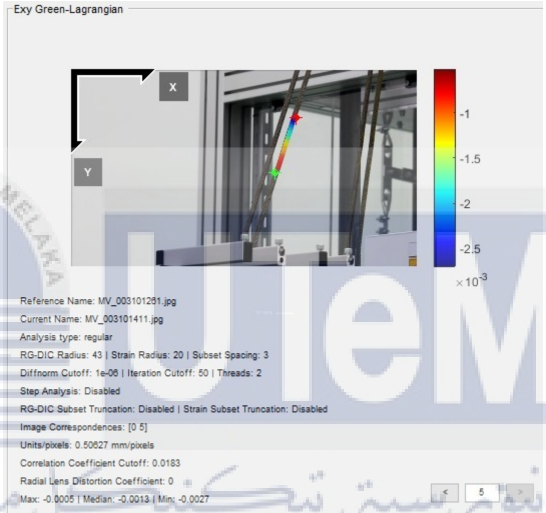 Reference Name: MV_003101261.jpg Current Name: MV_003101411.jpg Analysis type: regular RG-DIC Radius: 43 | Strain Radius: 20 | Subset Spacing: 3 Diffnorm Cutoff: 1e-06 | Iteration Cutoff: 50 | Threads: 2 Step Analysis: Disabled RG-DIC Subset Truncation: Disabled | Strain Subset Truncation: Disabled Image Correspondences: [0 5] Units/pixels: 0.50627 mm/pixels Correlation Coefficient Cutoff: 0.0183 Radial Lens Distortion Coefficient: 0 Max: -0.0005 | Median: -0.0013 | Min: -0.0027

4.2.2 Validation distance different between real image and Matlab value.

Table 4.3 Real Data Value

	REAL IMAGE (mm)
First image	27.00
Last image	46.84

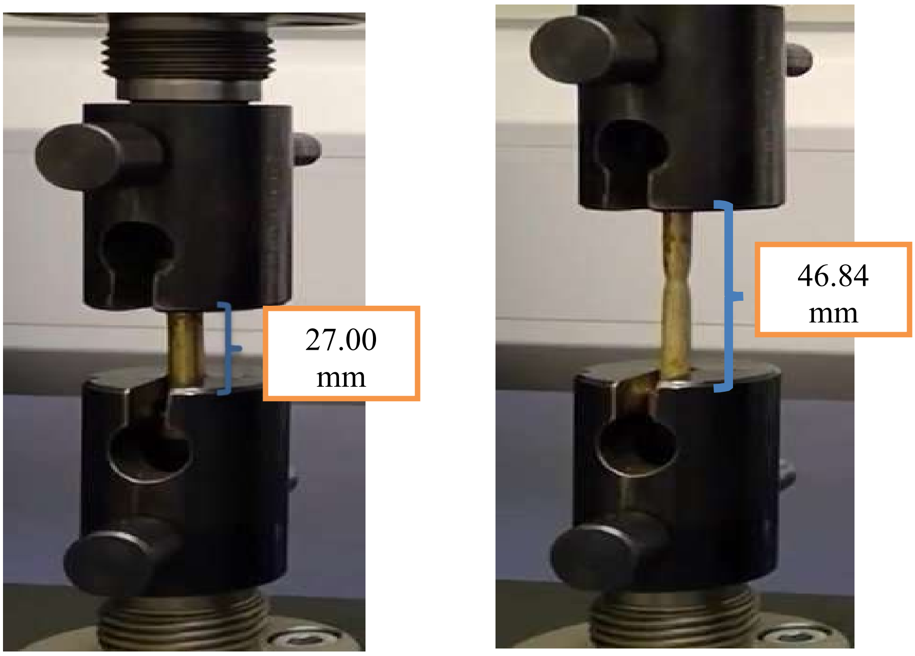

Figure 4.1 First and last real image

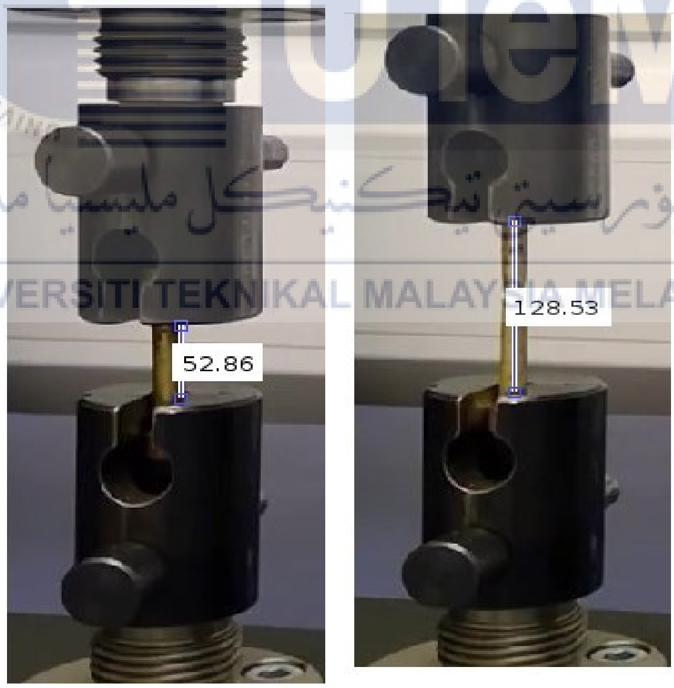

Figure 4.2 MatLab Data

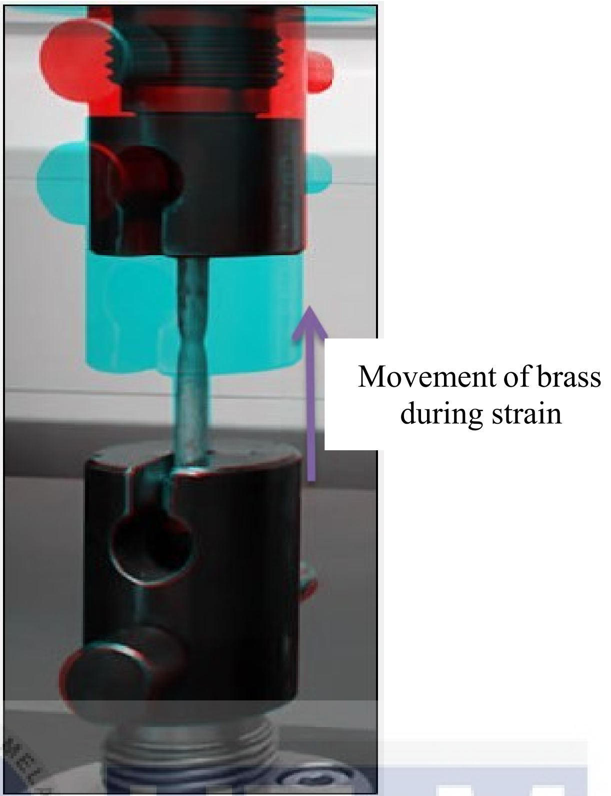

Movement of brass during strain

Figure 4.3 Overlay Image

DATA CALCULATION

Calculation:

Triangle Similarity:

$$F = \frac{(P \times D)}{W} \qquad [4]$$

where, F = focal length

P = apparent width/height in pixels

D = distance camera from the object

W = real width/height of the object

FIRST IMAGE:

$$F = \frac{(52.86pixel \times 40.00mm)}{27.00mm}$$

$$F = 78.31pixel$$

$$Distance\ of\ object = \frac{focal\ length \times real\ distance\ of\ the\ object \times image\ distance}{object\ distace \times sensor\ height}$$

$$40mm = \frac{78.31pixel \times 27.00mm \times 52.86pixel}{Object\ distance \times (97)}$$

$$Object\ length = 28.81\ mm$$

Table 4.4 Focal and Object length

	Focal length(pixel)	Object length(mm)
FIRST IMAGE	78.31	28.81
LAST IMAGE	109.76	48.94

Table 4.5 Data Comparison

	REAL DATA	MATLAB DATA
FIRST IMAGE	27.00	28.81
LAST IMAGE	46.84	48.94

Percentage:

$$\% = \frac{real\ data}{matlab\ data} \times 100$$

[5]

Table 4.6 Percentage

	Percentage (%)
FIRST IMAGE	93.72
LAST IMAGE	95.71

Average percentage:

$$\frac{93.72 + 95.71}{2} = \mathbf{94.72}\%$$

The average true value percentage according to the MatLab statistics is 94.72%. (which it is can be considered as mostly success for the validation of real image using MatLab software). The accuracy of the data increases with the value percentage. One inaccuracy that could result in a different outcome is when a measurement in MatLab's point-to-point mode is not aligned, which would result in a different measurement of the value and a lower percentage.

The correlation of digital images is employed for strain analysis. The digital image is easier to analyse than any other type of examination, such a strain gauge. A common technique for calculating the strain on an object is the strain gauge. It requires a strain gauge, often measured using a Wheatstone bridge that is related to the strain, that works on the principle of resistance change. Although purchasing the equipment (high speed camera) will be more expensive initially, the subsequent job will be lot simpler. The image of the data will be analysed as it is being collected using software (MatLab and Ncorr), which may be downloaded from the website.

CHAPTER 5

CONCLUSION AND RECOMMENDATIONS

5.1 Conclusion

From the objective that been stated earlier, high speed camera are obtain to take the image or video for the analysis in this research. High speed camera that been used are been put on the horizontal with the tools(cable/brass) to record the changes that happen on the cable and brass when force are been put on it. In addition, to analyse the analysis of strain and also the validation of data, the Matlab and Ncorr software are been used to proof the concept.

There were so many method that can be used for the analysis, but the Matlab were much better due to the accessibility of the software is much better compare to others. Compare to moire method in the literature review earlier, principle of in-plane moire method is a principle that is related to moire method(scar field p of each Moire edge represents the displacement p, with the frequency of the scar determining the sensitivity to each displacement).

This study can be continued after stating the problem and the goal at the outset by conducting numerous literature reviews to support the decision to use MatLab and Ncorr to conduct strain analysis. The validation process is then utilized to demonstrate the reliability of the cable's manufacturing method. To complete the Matlab process, good data will be collected. After a thorough analysis, a report will be written.

5.2 Recommendations

For future improvements, accuracy of the strain estimation results could be enhanced as follows:

i) By analyze the data for the real time cable instead of in the laboratory analysis

ii) Comparing the real data strain graph(theory) with the data taken in real life situation.

REFERENCES

A. F. Ab Ghani, M. B. Ali, S. Dharmalingam, & J. Mahmud. (2016). Digital Image Correlation (DIC) Technique in Measuring Strain Using Opensource Platform Ncorr. *Journal of Advanced Research in Applied Mechanics*, *26*(1), 10–21.

Ahmad, A., & Fırıncıoğlu, B. S. (2020). *Utilizing DIC Technique for Visualizing the Failure Modes of Concrete Specimens*. *10*(2). https://doi.org/10.19080/CERJ.2020.10.555783

Analysis, A. E. (2018). *Introduction to Finite-element Analysis* (Vol. 2018, Issue Isbn 9781119071204).

Andrés, N., Andres-Arroyo, A., Pilar Arroyo, M., Palero, V. R., Lobera, J., & Angurel, L. A. (2013). Application of digital speckle interferometry to visualize surface changes in metallic samples immersed in Cu(NO3)2 solutions. *Optical Engineering*, *52*(10), 101918. https://doi.org/10.1117/1.oe.52.10.101918

Aydin, M., Wu, X., Cetinkaya, K., Yasar, M., & Kadi, I. (2018). Application of Digital Image Correlation technique to Erichsen Cupping Test. *Engineering Science and Technology, an International Journal*, *21*(4), 760 – 768. https://doi.org/10.1016/j.jestch.2018.06.004

Brooks, R. E. (1969). Holographic Interferometry. *IEEE Journal of Quantum Electronics*, *5*(6), 360. https://doi.org/10.1109/JQE.1969.1081973

Cubreli, G., Psota, P., Dančová, P., Lédl, V., & Vít, T. (2021). Digital holographic interferometry for the measurement of symmetrical temperature fields in liquids. *Photonics*, *8*(6). https://doi.org/10.3390/photonics8060200

Davila, A. L. (2020). *Finite Element Analysis History of FEA 3 . 1 Discretization Strategy : Finite Elements*. 1–12.

Dhirubhai, A. R., Ratan, A., & Gatiyala, R. (2015). *Holography-Working Principle and Applications Holography Working Principle and Applications*. *April*. https://doi.org/10.13140/RG.2.1.2688.4649

Eichhorn, G. N. (2019). *Low-cost digital image correlation and strain measurement for geotechnical applications*.

Eindhoven, T. H., Produktietechnologie, V., Eindhoven, T. U., & Version, D. (2022). *An introduction to Moiré method*. *1992*.

Federal, U., Catarina, D. S., Viotti, M. R., Division, O. M., Ltda, P., Methods, H., &Methods, S. (n.d.). *Holographic and speckle methods*. 1–51.

Felippa, C. A. (2004). A compendium of FEM integration formulas for symbolic work. *Engineering Computations (Swansea, Wales)*, *21*(8), 867–890. https://doi.org/10.1108/02644400410554362

Górszczyk, J., Malicki, K., & Zych, T. (2019). Application of digital image correlation (DIC) method for road material testing. In *Materials* (Vol. 12, Issue 15). https://doi.org/10.3390/ma12152349

Hossack, W. (1998). *Topic 9: Holographic Interferometry*. 1–17.

Jagota, V., Sethi, A. P. S., & Kumar, K. (2013). Finite element method: An overview. *Walailak Journal of Science and Technology*, *10*(1), 1–8.

Lonetti, P., & Pascuzzo, A. (2016). A numerical study on the structural integrity of self-anchored cable-stayed suspension bridges. *Frattura Ed Integrita Strutturale*, *10*(38), 359–

376. https://doi.org/10.3221/IGF-ESIS.38.46

Low-cost digital image correlation and strain measurement for geotechnical applications _ Enhanced Reader.pdf. (n.d.).

McCormick, N., & Lord, J. (2010). Digital image correlation. *Materials Today*, *13*(12), 52–54. https://doi.org/10.1016/S1369-7021(10)70235-2

Melin, L. G. (1995). *Moiré Technique for Measurement of the Deformation Field at Crack Tips in Fiber Composite Materials*. *1995*(111).

Motamedi, M. A. (2019). *Introduction To DIC Technique*. *December*.

Mousa, M. A., Yussof, M. M., Udi, U. J., Nazri, F. M., Kamarudin, M. K., Parke, G. A. R., Assi, L. N., & Ghahari, S. A. (2021). *Application of Digital Image Correlation in Structural Health Monitoring of Bridge Infrastructures : A Review*.

Slangen, P., Berwart, L., De Veuster, C., Golinval, J. C., & Lion, Y. (1996). Digital Speckle Pattern Interferometry (DSPI): A fast procedure to detect and measure vibration mode shapes. *Optics and Lasers in Engineering*, *25*(4 – 5), 311 – 321. https://doi.org/10.1016/0143-8166(95)00078-X

Tavares, P. J. (2015). *SIF Determination with Digital Image Correlation*.

Terán-Guillén, J., Cicero, S., García, T., Alvarez, J. A., Martínez-Madrid, M., & Pérez-Quiroz, J. T. (2014). Structural integrity assessment of the cast steel upper anchorage elements used in a cable stayed bridge. *Engineering Structures*, *81*(December), 309 – 317. https://doi.org/10.1016/j.engstruct.2014.10.018

Workflow, A. (2018). *Structural Integrity Analyses of Dynamic Power Cables*.

APPENDICES

APPENDIX A GANTT CHART

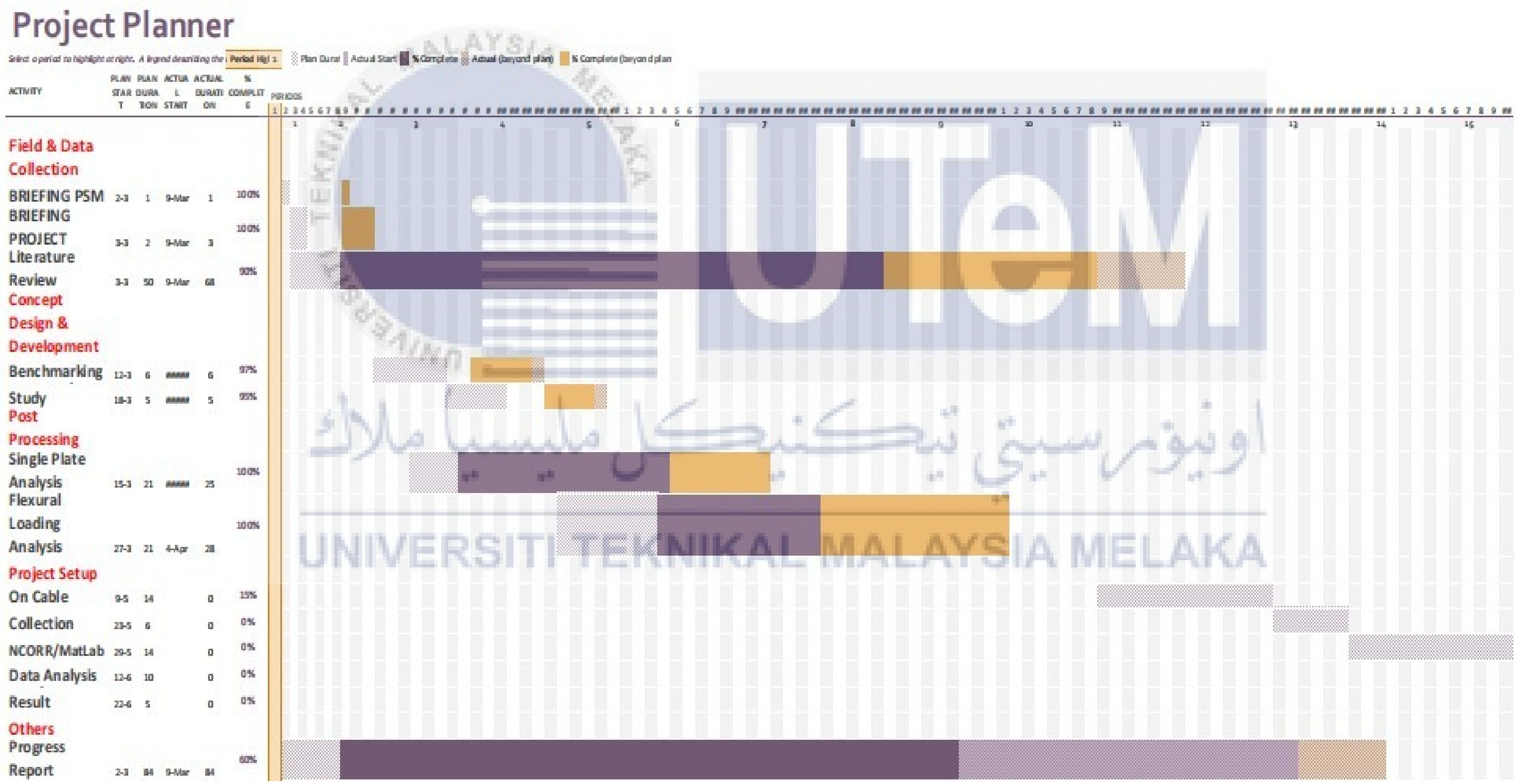

Project Planner

Select a period to highlight at right. A legend describing the Period Hig 1 ▨ Plan Durat ▨ Actual Start ■ % Complete ▨ Actual (beyond plan) ■ % Complete (beyond plan

ACTIVITY	PLAN START	PLAN DURATION	ACTUAL START	ACTUAL DURATION	% COMPLETE
Field & Data Collection					
BRIEFING PSM	2-3	1	9-Mar	1	100%
BRIEFING PROJECT	3-3	2	9-Mar	3	100%
Literature Review	3-3	50	9-Mar	68	90%
Concept Design & Development					
Benchmarking	12-3	6	#####	6	97%
Study	18-3	5	#####	5	95%
Post Processing					
Single Plate Analysis	15-3	21	#####	25	100%
Flexural Loading Analysis	27-3	21	4-Apr	28	100%
Project Setup					
On Cable	9-5	14		0	15%
Collection	23-5	6		0	0%
NCORR/MatLab	29-5	14		0	0%
Data Analysis	12-6	10		0	0%
Result	22-6	5		0	0%
Others					
Progress Report	2-3	84	9-Mar	84	60%